Clinical Science (2023) **137** 847–862
https://doi.org/10.1042/CS20220880

Research Article

NPFFR2-deficient mice fed a high-fat diet develop strong intolerance to glucose

Alena Karnošová[1,2,*], Veronika Strnadová[1,*], Blanka Železná[1], Jaroslav Kuneš[1,3], Petr Kašpárek[4] and Lenka Maletínská[1]

[1] Biochemistry and molecular biology, Institute of Organic Chemistry and Biochemistry of the Czech Academy of Sciences, 16610 Prague, Czech Republic; [2]First Faculty of Medicine, Charles University, 12108 Prague, Czech Republic; [3]Experimental hypertension, Institute of Physiology of the Czech Academy of Sciences, 14200 Prague, Czech Republic; [4]Czech Centre for Phenogenomics, Institute of Molecular Genetics of the Czech Academy of Sciences, Vestec 25250, Czech Republic

Correspondence: Lenka Maletínská (maletin@uochb.cas.cz)

A previous study on neuropeptide FF receptor 2 (NPFFR2)-deficient mice has demonstrated that NPFFR2 is involved in the control of energy balance and thermogenesis. Here, we report on the metabolic impact of NPFFR2 deficiency in male and female mice that were fed either a standard diet (STD) or a high-fat diet (HFD) and each experimental group consisted of ten individuals. Both male and female NPFFR2 knockout (KO) mice exhibited severe glucose intolerance that was exacerbated by a HFD diet. In addition, reduced insulin pathway signaling proteins in NPFFR2 KO mice fed a HFD resulted in the development of hypothalamic insulin resistance. HFD feeding did not cause liver steatosis in NPFFR2 KO mice of either sex, but NPFFR2 KO male mice fed a HFD had lower body weights, white adipose tissues, and liver and lower plasma leptin levels compared with their wild-type (WT) controls. Lower liver weight in NPFFR2 KO male mice compensated for HFD-induced metabolic stress by increased liver PPARα and plasma FGF21 hepatokine, which supported fatty acid β-oxidation in the liver and white adipose tissue. Conversely, NPFFR2 deletion in female mice attenuated the expression of *Adra3*β and *Ppar*γ, which inhibited lipolysis in adipose tissue.

Introduction

Neuropeptide FF (NPFF) belongs to the RF-amide peptide family, which is characterized by their conserved Arg-Phe-NH_2 sequence in the C-terminus. Although NPPF was originally found to regulate nociception, multiple studies have implicated its ability to reduce food intake in rodents or chicks after intracerebroventricular injection [1–4]. NPFF has recently been reported to directly control glucose homeostasis, and the deletion of NPFF improves glucose tolerance and lowers blood glucose levels in mice fed a high-fat diet (HFD) without any effect on blood insulin levels [5]. NPFF may influence glucose homeostasis by affecting the β-adrenergic system, which not only activates lipolysis and thermogenesis but also negatively controls lipogenesis and glucose transport [6].

NPFF acts through the G-protein coupled receptors, NPFFR1 (GPR147) and neuropeptide FF receptor 2 (NPFFR2; GPR74), but it shows higher affinity and activity toward NPFFR2. Another RF-amide peptide, prolactin-releasing peptide (PrRP), binds with high affinity to and activates not only its receptor, GPR10, but also NPFFR2 and NPFFR1 [7]. The receptors of other food intake-regulating peptides, such as orexin, neuropeptide Y (NPY), cholecystokinin, and PrRP, share high amino acid sequence homology with NPFFR2. Moreover, the human *Npffr2* gene is localized near the gene cluster of the NPY receptors, Y5, Y1, and Y2, on chromosome 4q31, suggesting its importance in energy homeostasis and regulation of food intake. Additionally, it has been discovered that NPFFR2 signaling plays a significant role in maintaining the basal expression of NPY [8–10].

NPFF and both NPFFR2 and NPFFR1 are highly expressed in the central nervous system (CNS), and NPFFR2 expression is more abundant than NPFFR1 expression in the CNS [8,11]. The highest density

[*]These authors contributed equally to this work.

Received: 04 January 2023
Revised: 15 May 2023
Accepted: 16 May 2023

Accepted Manuscript online: 16 May 2023
Version of Record published: 31 May 2023

Clinical Science (2023) **137** 847–862
https://doi.org/10.1042/CS20220880

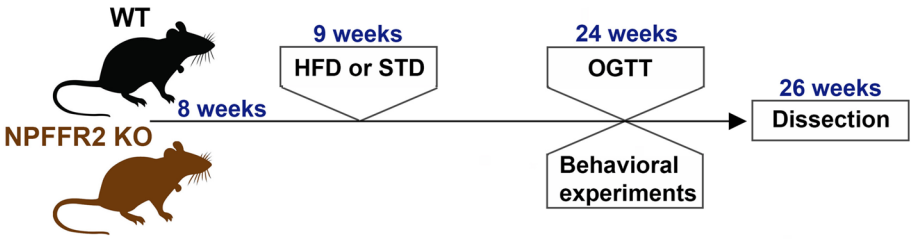

Figure 1. Experimental design

of NPFFR2 exists in the amygdala, spinal cord, and dorsomedial hypothalamic nucleus. Lower NPFFR2 expression is present in various regions of the hypothalamus, such as the paraventricular nucleus, ventromedial nucleus, or lateral hypothalamus [8,12–14]. Even though NPFF and NPFFR2 are expressed predominantly in the CNS, high *Npffr2* mRNA expression is detected in the placenta and adipose tissue, and low levels of mRNA are found in the heart, kidney, or lung in rats [8]. Recently, Waqas et al. reported that NPFFR2, but not NPFFR1, is expressed in human and mouse white adipose tissue macrophages, which may influence the development of obesity-induced metabolic diseases [15].

When fed a HFD, it has been shown that NPFFR2 deficiency results in the development of obesity associated with a failure to activate brown adipose tissue (BAT) as well as decreased thermogenesis and significantly lowered mRNA expression of uncoupling protein-1 (UCP1) in BAT [9]. This finding demonstrates that HFD-induced adaptive thermogenesis is dependent on functional NPFFR2 signaling. NPFFR2 receptor colocalization with NPY neurons indicates the importance of NPFFR2 signaling in the regulation of the NPY system. Moreover, NPY expression in the arcuate nucleus is significantly down-regulated in NPFFR2 knockout (KO) mice, resulting in the inability to regulate energy balance in mice fed a HFD [9].

In our previous studies, we reported that PrRP and its palmitoylated analogs bind with a high affinity to both GPR10 and NPFF2 receptors [16,17]. Palmitoylation of PrRP increased its stability and enabled PrRP to accomplish its central anorexigenic effect after peripheral administration [18]. After producing and characterizing GPR10 KO mice [19], we produced NPFFR2 KO mice in order to distinguish participation of the particular receptors in anorexigenic and antidiabetic effects of palmitoylated PrRP analogs. In the present study, metabolic phenotyping was performed with NPFFR2-deficient and age-matched wild-type (WT) control mice (both males and females at the age of 6 months) fed a standard diet (STD) or HFD. Strong glucose intolerance was observed in NPFFR2 KO mice, which was exacerbated by an HFD diet. In NPFFR2-deficient mice, HFD worsened insulin signaling in the hypothalamus and brainstem, and it induced liver metabolic stress and impacted lipid metabolism in adipose tissue.

Materials and methods

Animals and experimental design

Mice carrying a null mutation in the *Npffr2* gene (Supplementary Figure 1) were generated in Czech Centre for Phenogenomics, Institute of Molecular Genetics of the Czech Academy of Sciences, Czech Republic on a C57BL/6N background using a CRISPR genome-editing system. Specific guide RNAs (gRNAs) recognizing Npffr2 exon 2 (5′-CCAGTAAATCACTTATGGCA -3′ and 5′-ATGAAGACAGCTGCCACTTG -3′) were designed, and off-target analyses were performed using the online CRISPOR design tool. spCas9 protein (500 ng/μl) and gRNAs (50 ng/μl each) were used for zygote electroporation according to a previously described protocol [20]. The correct genome editing was confirmed by PCR amplification in the founder mice using the following primers: Npffr2-F, 5′-CTTCCGATGTCCACCTGTCT-3′; and Npffr2-R, 5′-GGTGGTACCAGCGAAGTGAT-3′.

The animals (n=80 in total) were handled in accordance with good animal practices, and all experiments were approved by the Committee for Experiments with Laboratory Animals of the Czech Academy of Sciences and followed the ethical guidelines for animal experiments as provided in the Czech Republic Act Nr. 246/1992. All animals experiments took place in the Animal Facility of the Institute of Organic Chemistry and Biochemistry, Czech Academy of Sciences (CAS), Prague, Czech Republic. The animals were housed under controlled conditions at 22°C and under a 12 h light cycle (lights on at 6:00 a.m.). Mice had free access to water and a STD (Ssniff R/M-H diet; 8% kcal from fat, 21% kcal from protein, and 71% kcal from carbohydrate; Ssniff Spezialdieten GmbH, Soest, Germany).

Mice of both sexes and genotypes were exposed to either a STD or HFD (60% kcal from fat, 13% kcal from protein, and 27% kcal from carbohydrate [21]) from the age of 9 weeks (Figure 1). In each experimental group, the sample size

of mice was comprised of ten individuals, with n=10. At the end of the experiment at 26 weeks of age, tail blood was collected for plasma leptin detection. The mice in a randomly fed state were deeply anesthetized with pentobarbital (120 mg/kg of body weight, Sigma–Aldrich, St. Louis, MO, U.S.A.) and transcardially perfused with ice-cold 0.01 M phosphate-buffered saline (PBS) pH 7.4 supplemented with heparin (20 U/ml, Zentiva, Prague, CzechRepublic). Interscapular BAT, subcutaneous white adipose tissue (scWAT), gonadal white adipose tissue (gWAT), the liver, the hypothalamus, and the brainstem were dissected. Tissue samples were frozen in liquid nitrogen and then stored at −80°C until further analysis. Samples were evaluated by morphometric analysis, biochemical analysis, liver histology, western blot analysis, and mRNA analysis.

Behavioral experiments and nociception

Male and female mice on a STD or HFD at 24 weeks of age (Figure 1) were subjected to the open field (OF) test and elevated plus maze (EPM) to assess locomotor activity, exploration of a novel environment, and anxiety-like behavior. Nociception (pain sensitivity) was determined by a hot plate (HP) test. The experiments were conducted between 8:00 a.m. and 12:00 p.m. to minimize the influence of circadian fluctuations, despite the fact that it was during the sleep phase of the mice. The surfaces of the mazes were wiped with 70% ethanol after each measurement to eliminate odor trails.

OF test

Mice were placed individually in the corner of the square arena (50 × 50 cm), and their locomotor activity was recorded for 10 min [22]. We designed the central area square as half of the size of the arena to track time spent and the number of entries in the central area to measure anxiety-like behavior and tendency to explore open areas. The total track length was monitored. The obtained record was analyzed using EthoVision XT software (Noldus, Wageningen, Netherlands).

EPM

Mice were placed individually in the center of the maze, and their activity was recorded for 10 min. The time spent in the arms and the number of entries into the open or closed arms was calculated using EthoVision XT software.

HP test

The pain threshold to thermal stimulation was measured using a HP system (TSE Systems, Bad Homburg, Germany) set at 53°C. The HP latency was defined as the period between placing the animal on the HP surface and the occurrence of nociceptive behavior (front paw licking). After every trial session, the mice were immediately removed from the plate and returned to the cage.

Determination of the mRNA expression of genes in the brain and organs

Samples from the BAT, scWAT, gWAT, and liver were processed as previously described [23]. Samples were analyzed from WT and NPFFR2 KO mice of both sexes fed either a STD or HFD (n=4–5), and the mRNA expression of genes of interest (Supplementary Table 1) was determined using an ABI PRISM 7500 instrument (Applied Biosystems, Foster City, CA, U.S.A.). The expression of beta-2-microglobulin (*b2M*) was determined for variations in the amounts of input RNA and normalization of the efficiency of reverse transcription. All mRNA probes were purchased from Thermo Fisher Scientific (MA, U.S.A.).

Oral glucose tolerance test

The oral glucose tolerance test (OGTT) was performed in 24-week-old (Figure 1) WT and NPFFR2 KO mice of both sexes and diets after 6 h of fasting. At 0 min, fasted blood was collected from the tail veins to assess the levels of insulin, glucagon, triacylglycerol (TAG), free fatty acid (FFA), cholesterol, and fibroblast growth factor 21 (FGF21), and glucose at a dose of 2 g/kg of body weight was administered orally by gavage. Blood glucose concentrations in the whole blood were determined at 15, 30, 60, 90, 120, and 180 min after glucose gavage using a glucometer (LifeScan, Inc., Milpitas, CA, U.S.A.).

Biochemical analyses of the plasma

Fasted plasma was used to detect insulin and glucagon using radioimmunoassays (Millipore Sigma, Burlington, MA, U.S.A.). FFA (Roche, Mannheim, Germany), FGF21 (Millipore Sigma), and cholesterol with TAG (Erba Lachema, Brno, Czech Republic), were detected using using a colorimetric assay. Free-fed plasma was used to detect leptin (Millipore Sigma).

Clinical Science (2023) **137** 847–862
https://doi.org/10.1042/CS20220880

Hematoxylin and eosin staining of the liver

The right lobe of the liver was fixed in 4% PFA, embedded in paraffin, and cut into sections with a 5-μm thickness. Liver sections were processed as previously described [19]. The samples were covered with DPX mounting medium (Millipore Sigma), and representative photomicrographs of the liver sections were acquired using an Olympus IX83 microscope (Olympus Europa SE & Co. KG, Hamburg, Germany).

Western blot analysis

Samples from the hypothalamus, brainstem, and liver were processed and stored at −20°C. Western blot analysis was performed as previously described [24]. Membranes were blocked for 1 h and then incubated with primary antibodies (Supplementary Table 2) overnight at 4°C. The protein level was normalized to glyceraldehyde 3-phosphate dehydrogenase (GAPDH).

Statistical analysis

Differences between WT or NPFFR2 KO mice on either a STD or HFD were statistically analyzed by ordinary one-way or two-way ANOVA with Bonferroni post hoc test using GraphPad Prism 8 software (GraphPad Software, Inc., San Diego, CA, U.S.A.). Data are presented as the mean ± SEM and assume normal (Gaussian) distribution of data.

Results

Generation and validation of NPFFR2 KO mice

We used CRISPR/Cas9 technology to generate mice carrying a mutation in exon 2 of the *Npffr2* gene. PCR genotyping revealed a founder mouse carrying 137 bp deletion in Npffr2 coding sequence (Supplementary Figure 1A) leading to a frameshift and premature STOP codon, presumably resulting in a nonfunctional protein product. Germ-line transmission of the null mutation (Supplementary Figure 1B) allowed the establishment of NPFFR2 KO mouse line.

NPFFR2 deletion does not alter behavior or pain perception

NPFFR2 KO and WT mice were tested using OF and EPM tests to identify potential changes in behavior (Figure 2). The track length traveled in the OF arena was comparable in WT and NPFFR2 KO mice (Figure 2A–D). NPFFR2 KO mice and their WT controls on a HFD tended to explore less, and they avoided open areas in the OF (Figure 2A–H). NPFFR2 KO male mice did not reveal any anxiety-like behavior in either the OF or EPM (Figure 2A,B,E,F,I,J,M). NPFFR2 KO females, but not males, fed a HFD spent significantly more time in the junction area of the EPM than those fed a STD (Figure 2L). In addition, NPFFR2 KO mice exhibited unaltered pain perception in the HP test compared with WT mice (Figure 2N,P).

STD-fed NPFFR2 KO mice exhibit a lean phenotype, and HFD-fed NPFFR2 KO males gain less weight than their WT controls

On a standard chow diet, NPFFR2 KO mice, both males and females, displayed a growth curve similar to that of WT mice (Figure 3A,G). The HFD was started from the 9th week of age, and body weight and food intake were monitored. The HFD significantly increased body weight in both NPFFR2 KO and WT mice (Figure 3A,B,G,H). However, HFD-fed NPFFR2 KO males, but not females, had significantly lower body weights compared with their WT controls (Figure 3B,H).

Dissected organs were weighed at the end of the experiment when mice were 6 months old in a freely fed state. The weights of both adipose tissues dissected (scWAT and gWAT) (Figure 3D,J) followed the body weight trend (Figure 3B,H) in all mice. HFD-fed NPFFR2 KO males, but not females, had significantly lower weights of both adipose tissues (Figure 3B,D) compared with their WT controls.

As expected, HFD generally caused a significant increase in plasma leptin levels (Figure 3E,K) and *leptin* mRNA expression (Figure 3F,L). However, HFD-fed NPFFR2 KO mice had a lower leptin level than WT control mice (Figure 3E), which was in line with the body weights and adipose tissue weights.

The HFD increased plasma cholesterol and TAG in both NPFFR2 KO and WT mice (Table 1). NPFFR2 KO females fed a STD had lower plasma cholesterol and TAG levels than their WT controls (Table 1). Plasma FFA did not differ among groups (Table 1).

Complete morphometric analysis in NPFFR2 KO and WT mice at 26 weeks and plasma metabolic profile at 24 weeks is described in Supplementary Table 3.

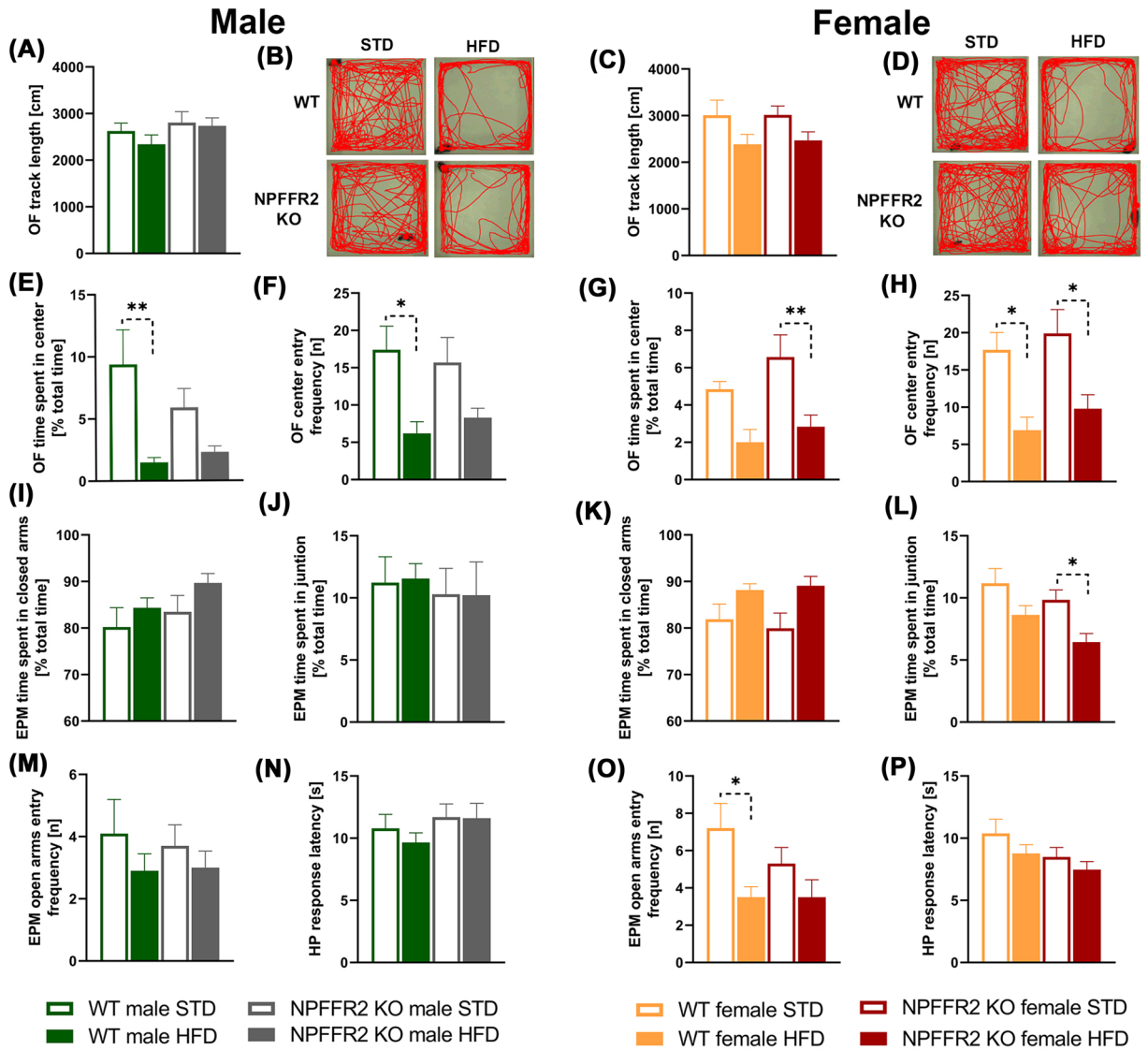

Figure 2. Behavioral experiments and pain perception of NPFFR2 KO and WT mice

Impact of NPFFR2 deletion on behavioral changes in locomotor activity and anxiety-like behavior in the OF arena (**A–H**) and EPM (**I–M**,**O**). For the OF test, track length for (**A**) males and (**C**) in females, and track during the test for (**B**) males and (**D**) in females. Percentage (%) of time spent in the center zone (10 min total test time) for (**E**) males and (**G**) females, and the number of entries to the center zone for the (**F**) males and (**H**) females. For the EPM, percentage (%) of time spent in closed arms (10 min total test time) for (**I**) males and (**K**) females. Percentage (%) of time spent in the junction zone (10 min total test time) for (**J**) males and (**L**) females. Frequency of open arms visits for (**M**) males and (**O**) females. For the HP test, latency to pain perception (paw licking) for (**N**) males and (**P**) females. Data are expressed as the mean ± SEM (n=10) as determined by one-way ANOVA with Bonferroni post hoc test. *P<0.05 and **P<0.01 for HFD versus STD mice of the same genotype.

NPFFR2 KO mice have strong glucose intolerance enhanced by HFD and disrupted insulin signaling in the brain

Tolerance to glucose was determined by OGTT in NPFFR2 KO and WT mice of both sexes fed a STD or HFD. The fasted glucose before the OGTT was higher in HFD-fed WT mice of both sexes and NPFFR2 KO females than in their respective STD-fed controls (Figure 4C,H). As expected, fasted plasma insulin was higher in HFD-fed NPFFR2 KO and WT mice of both sexes (Figure 4D,I) than in their respective STD-fed controls. Interestingly, fasted plasma glucagon levels were lower in HFD-fed NPFFR2 KO females than in their WT controls (Figure 4J), but no significant difference was observed among the male groups (Figure 4E).

Clinical Science (2023) **137** 847–862
https://doi.org/10.1042/CS20220880

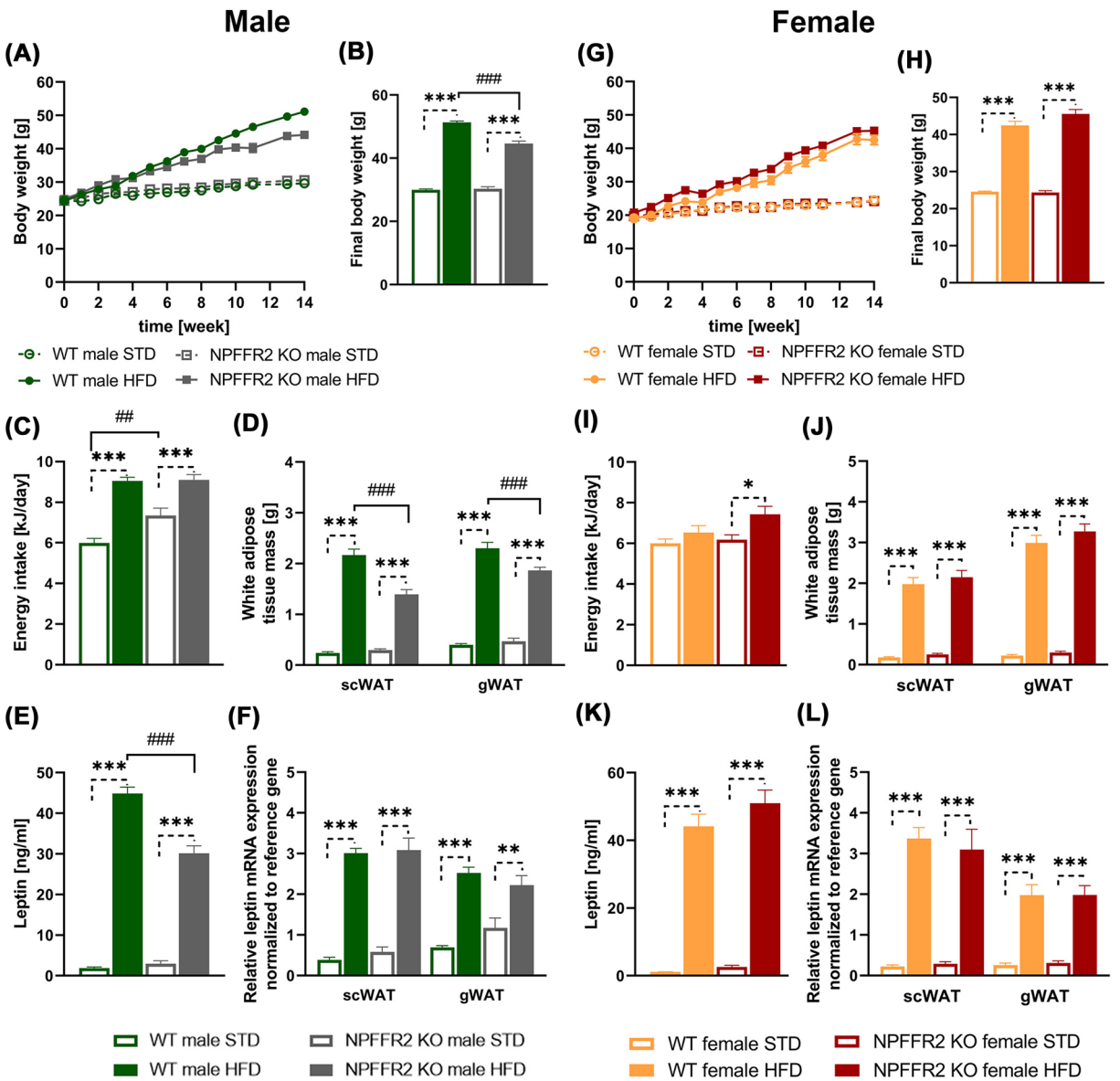

Figure 3. NPFFR2 KO mice reveal a lean phenotype on a STD, and males on a HFD show a lower BW than WT controls

Time course of body weight gain in (**A**) males and (**G**) females. Final body weight (**B,H**). Average energy intake of NPFF2 KO mice on a STD or HFD in (**C**) males and (**I**) females. Weights of dissected scWAT and gWAT in (**D**) males and (**J**) females. Serum leptin levels in (**E**) males and (**K**) females. All data are expressed as the mean ± SEM (n=10). mRNA expression of *leptin* in white adipose tissues in (**F**) males and (**L**) females. Data are expressed as the mean ± SEM (n=5). Data were determined by one-way ANOVA with Bonferroni post hoc test. *P<0.05, **P<0.01, and ***P<0.001 for HFD versus STD of the same genotype; ##P<0.01 and ###P<0.001 for NPFFR2 KO versus WT mice on the same diet.

Surprisingly, in the OGTT, NPFFR2 deficiency resulted in a higher area under the curve (AUC) in both HFD- and STD-fed mice of both sexes (Figure 4B,G). Furthermore, HFD-fed NPFFR2 KO mice showed substantially greater glucose excursions than their WT controls (Figure 4A,F). As expected, HFD-fed NPFFR2 KO mice of both sexes had a significantly higher AUC than their respective STD-fed controls (Figure 4B,G). Only HFD-fed WT males, but not females, had a higher AUC than mice fed a STD (Figure 4B,G). Severe glucose intolerance in NPFFR2 KO mice indicated potential insulin resistance in tissues.

Glucose intolerance in NPFFR2 KO mice negatively affected brain insulin signaling. HFD-fed NPFFR2 KO mice displayed significantly decreased hypothalamic insulin signaling proteins, namely, phosphoinositide 3-kinase (PI3K)

Table 1 Plasma metabolic profile of NPFFR2 KO and WT mice at 24 weeks of age

Group	TAG [mmol/l]	FFA [mmol/l]	Cholesterol [mmol/l]
WT male STD	0.45 ± 0.02	0.73 ± 0.10	1.95 ± 0.12
WT male HFD	0.54 ± 0.04	0.60 ± 0.04	3.98 ± 0.07 ***
NPFFR2 KO male STD	0.43 ± 0.03	0.57 ± 0.06	1.89 ± 0.12
NPFFR2 KO male HFD	0.55 ± 0.04 *	0.61 ± 0.06	3.87 ± 0.18 ***
WT female STD	0.45 ± 0.03	0.47 ± 0.06	3.36 ± 0.21
WT female HFD	0.58 ± 0.02 **	0.39 ± 0.03	5.49 ± 0.23 ***
NPFFR2 KO female STD	0.35 ± 0.01 #	0.44 ± 0.04	2.17 ± 0.18 ##
NPFFR2 KO female HFD	0.51 ± 0.04 ***	0.38 ± 0.04	6.14 ± 0.28 ***

Data are expressed as the mean ± SEM (n=8–10) as determined by one-way ANOVA with Bonferroni post hoc test. *P<0.05, **P<0.01, and ***P<0.001 for HFD versus STD of the same genotype; #P<0.05, ##P<0.01, and ###P<0.001 for NPFFR2 KO versus WT mice on the same diet. Abbreviations: TAG, triglyceride; FFA, free fatty acid.

regulatory subunit p85, PI3K regulatory subunit p110α, total protein kinase B (Akt), and total AS160 (Akt substrate), compared with their respective WT controls. In addition, the levels of p-AS160 (Ser588) in HFD-fed NPFFR2 KO males and p-Akt (Ser473) in HFD-fed NPFFR2 KO females were lower than those in their respective WT controls (Figure 5A,B). In the brainstem, insulin-signaling proteins in HFD-fed NPFFR2 KO males followed a similar trend as those in the hypothalamus (Figure 5A,C). In addition, insulin-signaling proteins, namely, PI3K regulatory subunit p85, p-Akt (Ser473), and p-AS160 (Ser588), were diminished in STD, but not HFD, fed NPFFR2 KO females compared with their WT controls (Figure 5D).

HFD-fed NPFFR2 KO mice do not develop fatty liver, and males produce FGF21 as a compensator for metabolic stress

The liver weights of NPFFR2 KO and WT mice fed a STD did not differ (Figure 6A,D). NPFFR2 KO males fed a HFD had a lower liver weight than their WT controls (Figure 6A), which was similar to their body weight (Figure 3B). The HFD significantly increased the liver weight in WT males and NPFFR2 KO females but not in NPFFR2 KO males or WT females (Figure 6A,D),

The liver histology for NPFFR2 KO and WT mice is shown in Figure 6C,F. There were no significant changes regarding the accumulation of fat droplets in the livers of NPFFR2 KO mice of both sexes fed a STD compared with their WT controls. The HFD increased the fat droplet area only in WT mice of both sexes (Figure 6B,E). Overall, deletion of NPFFR2 had no effect on lipid accumulation in the liver.

NPFFR2 deficiency in female mice indirectly affected hepatic insulin signaling even though the *Npffr2* gene was not expressed in the liver (Figure 6G,H). HFD-fed NPFFR2 KO females, but not males, displayed significantly decreased hepatic insulin-signaling proteins, namely, PI3K regulatory subunit p85, phosphoinositide-dependent protein kinase (PDK), and total Akt, compared with their WT controls (Figure 6H); in addition, p-Akt had a similar trend as total Akt but a nonsignificant outcome. As expected, the HFD lowered insulin signaling in NPFFR2 KO and WT mice of both sexes (Figure 6G,H).

The HFD did not affect total liver c-Jun NH2-terminal kinase (JNK) protein in WT males and females but caused a decrease in total JNK protein in both NPFFR2 KO males and females (Figure 7A,B). Generally, JNK negatively affects hepatic *Pparα* expression. A decrease in JNK expression in HFD-fed NPFFR2 KO males, but not females, may contribute to the increased hepatic PPARα protein (Figure 7A,B), and the *Pparα* mRNA gene expression had a similar trend as the protein expression (Figure 7C,D). PPARα acts as a transcription factor of the FGF21 hepatokine. Even though *Fgf21* mRNA expression was not elevated, FGF21 protein in fasted plasma was significantly elevated in HFD-fed NPFFR2 KO males compared with their WT controls (Figure 7E,F).

NPFFR2 KO affects adipose tissue mRNA expression of several genes involved in lipid metabolism

First, we compared BAT mRNA expression in NPFFR2 KO and WT mice of both sexes and diets. HFD-fed NPFFR2 KO males had decreased mRNA expression of *Vegfα* and *Tnfα* compared with their WT controls, while HFD-fed NPFFR2 KO females displayed significantly lower mRNA expression of *Prdm16* than their WT controls. Interestingly, the HFD augmented the mRNA expression of *Ucp1, Prdm16, Vegfα Pparγc1a, Adr3*β, and *Tnfα* in both

Clinical Science (2023) **137** 847–862
https://doi.org/10.1042/CS20220880

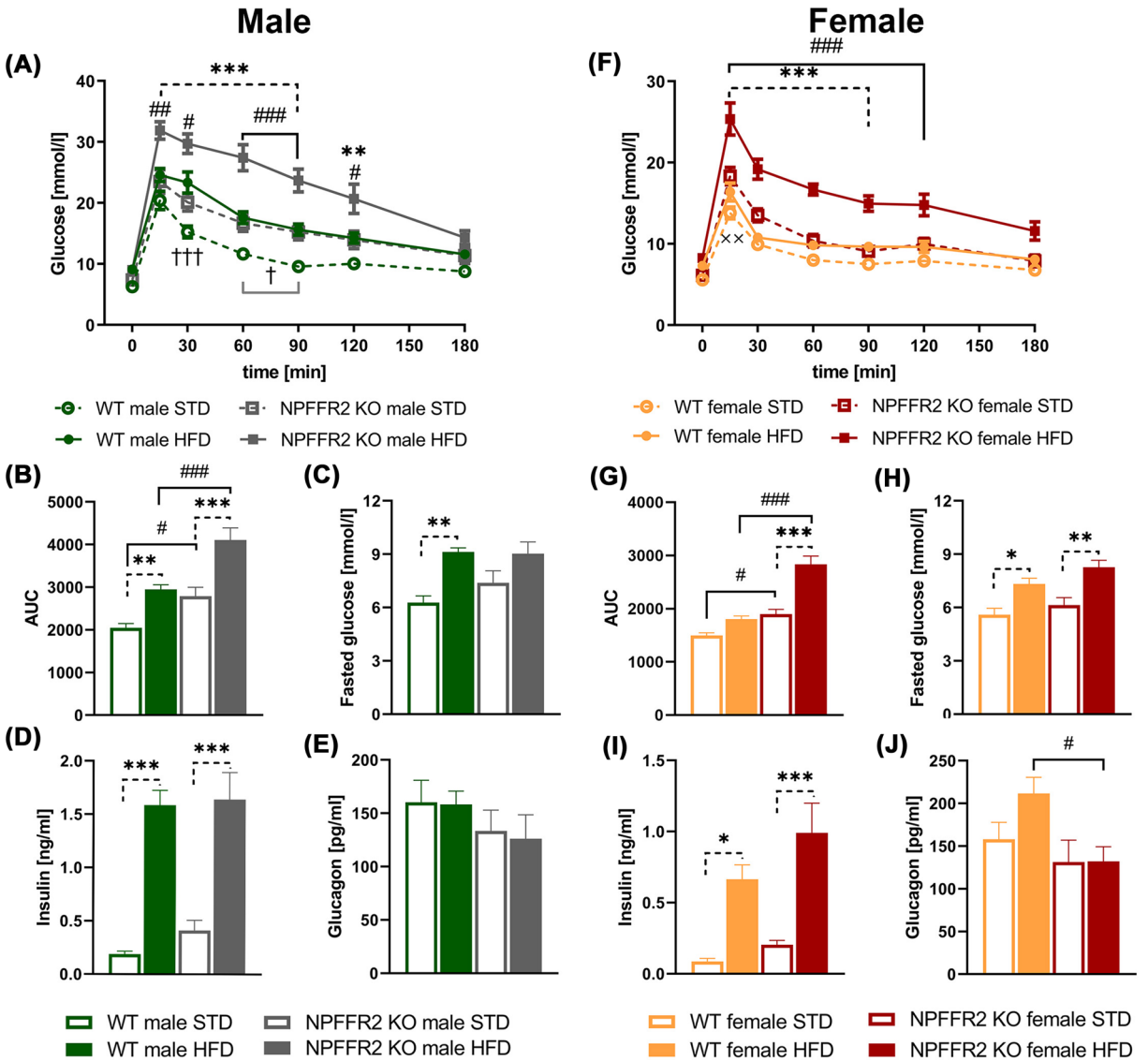

Figure 4. NPFFR2 KO mice fed a HFD have strong glucose intolerance

Blood glucose excursions in (**A**) males and (**F**) females after oral glucose gavage (dose 2 g/kg). OGTT data are expressed as the mean ± SEM (n=10) and were determined by two-way ANOVA with Bonferroni post hoc test. †P<0.05 and †††P<0.001 for WT mice fed a STD versus HFD; ××P<0.01 for NPFFR2 KO versus WT mice fed a STD; #P<0.05, ##P<0.01, and ###P<0.001 for WT mice versus NPFFR2 KO mice fed a HFD; **P<0.01 and ***P<0.001 for NPFFR2 KO mice fed a HFD versus NPFFR2 KO mice fed a STD. Area under the OGTT curves for (**B**) males and (**G**) females. Levels of fasted glucose in (**C**) males and (**H**) females. Fasted insulin levels in (**D**) males and (**I**) females. Fasted glucagon levels in (**E**) males and (**J**) females. Data are expressed as the mean ± SEM (n=7–10) and were determined by one-way ANOVA with Bonferroni post hoc test. #P<0.05, ##P<0.01, and ###P<0.001 for NPFFR2 KO versus WT mice on the same diet; *P<0.05, **P<0.01, and ***P<0.001 for HFD versus STD mice of the same genotype.

NPFFR2 KO and WT females, but the HFD only augmented the mRNA expression of *Tnfα* in males (Supplementary Figure 2A,B).

The impact of NPFFR2 deficiency on the mRNA expression of genes mostly involved in lipid metabolism in gWAT and scWAT is shown in Supplementary Figures 3 and 4, respectively. The HFD influenced the mRNA expression of most genes, but NPFFR2 deletion caused only a few changes. STD-fed NPFFR2 KO females displayed consistently lower mRNA expression of *Pparγ*, *adiponectin*, and *Adr3β* than their WT controls in both eWAT and scWAT (Supplementary Figures 3D,H and 4D,H). In the gWAT of STD-fed NPFFR2 KO males, the mRNA expression of the lipogenic genes, *Acaca* and *Fasn*, in the eWAT was higher compared with their respective WT controls, and there was

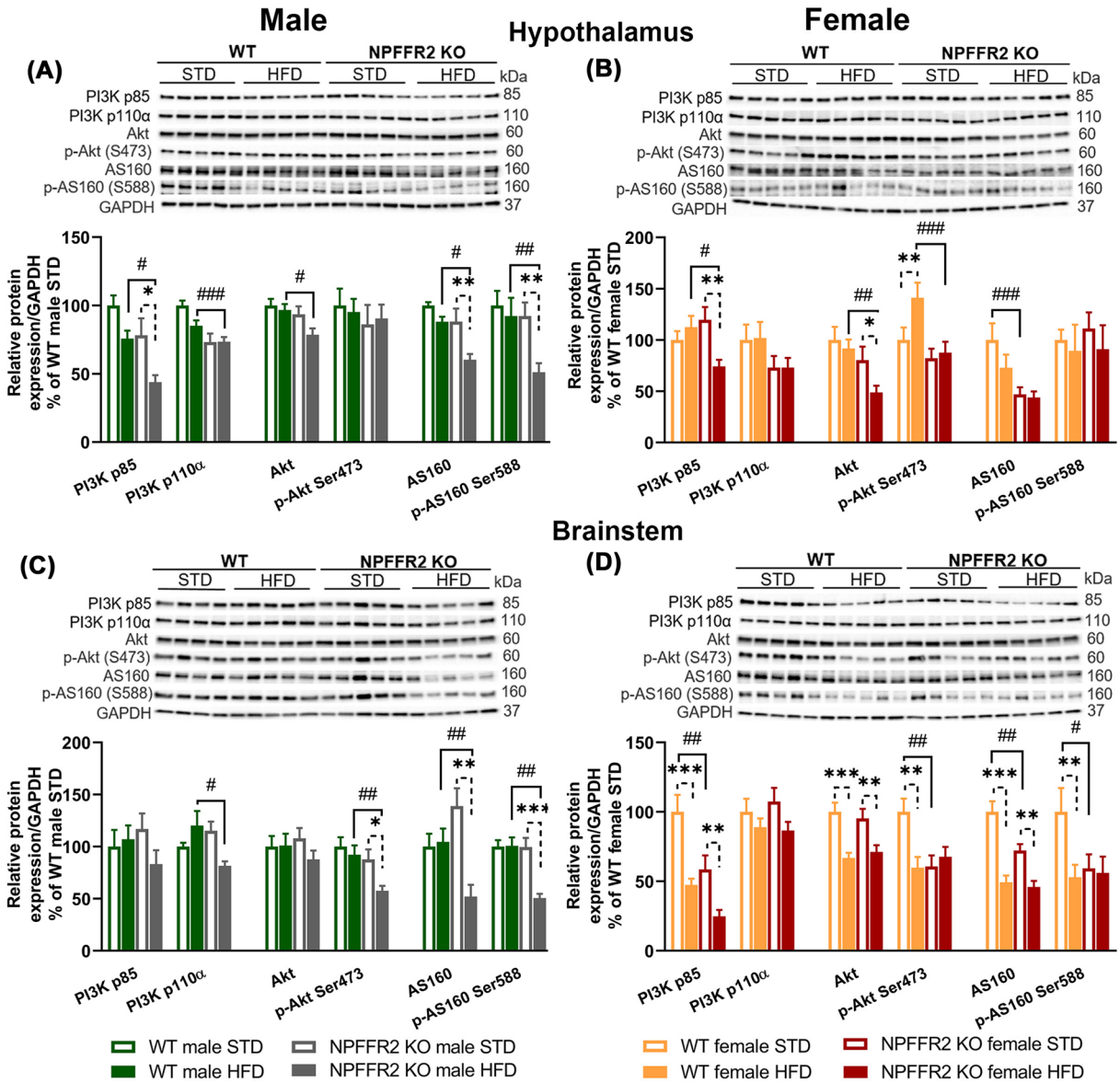

Figure 5. NPFFR2 KO mice fed a HFD have disrupted insulin signaling in the brain

WB analysis of hypothalamic (**A,B**) or brainstem (**C,D**) signaling. Densitometric quantification of the western blots normalized to GAPDH. Data are expressed as the mean ± SEM (n=4–5) and were determined by one-way ANOVA with Bonferroni post hoc test. #P<0.05, ##P<0.01, and ###P<0.001 for NPFFR2 KO versus WT mice on the same diet; *P<0.05, **P<0.01, and ***P<0.001 for HFD versus STD mice of the same genotype.

a lower *Tnfα* mRNA expression level in the eWAT in HFD-fed NPFFR2 KO males compared with their respective WT controls (Supplementary Figure 3E,G). In the scWAT of STD-fed NPFFR2 KO males, the *Pnpla2* mRNA expression was lower compared with their respective WT controls.

NPFFR2 KO only altered the liver expression of a few genes related to lipid metabolism regulation (Supplementary Figure 5). STD-fed NPFFR2 KO females had higher *Irs2* and lower *Hmgcs1* mRNA expression than their WT controls (Supplementary Figure 5). A low impact of the HFD on mRNA gene expression was observed with only a robust decrease in *Scd1* mRNA expression in both NPFF2R KO and WT males.

There were no changes found in GPR10 and NPFFR1 expression in hypothalami between genotypes (Supplementary Figure 6).

Clinical Science (2023) **137** 847–862
https://doi.org/10.1042/CS20220880

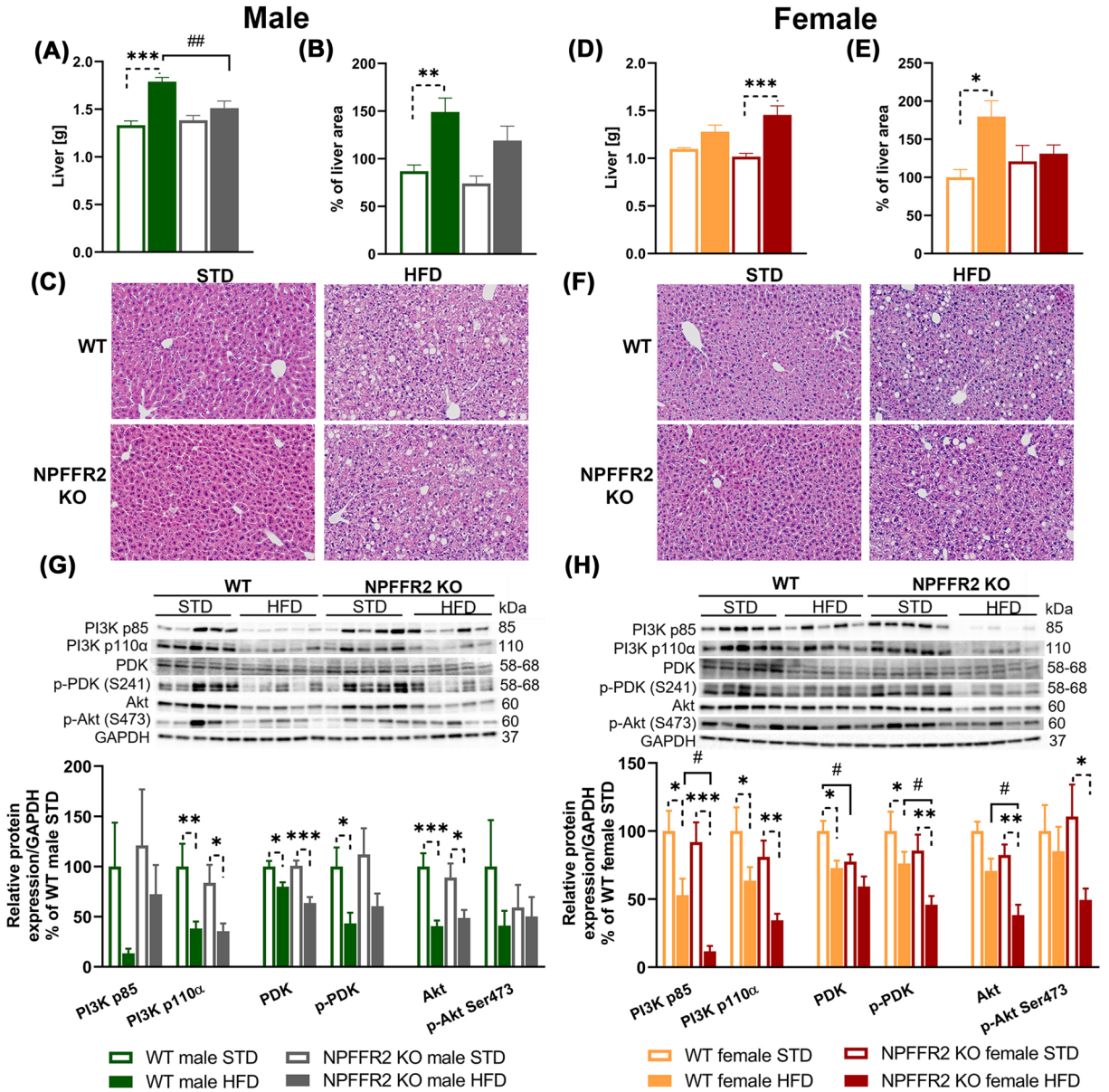

Figure 6. NPFFR2 KO mice do not show changes in liver histology but show worsened hepatic insulin signaling when fed a HFD

Weights of dissected liver in (**A**) males and (**D**) females. Data are expressed as the mean ± SEM (n=10). Liver histology quantification represented by percentage (%) of fat droplets in the liver area in (**B**) males and (**E**) females. Data are expressed as the mean ± SEM (n=4–5). Representative photomicrographs of H&E staining of liver sections with 200x magnification in (**C**) males and (**F**) females. Western blots of the insulin signal transduction pathway in (**G**) males and (**H**) females in the liver. Densitometric quantification of the western blots normalized to GAPDH. Data are expressed as the mean ± SEM (n=5). All data were analyzed by one-way ANOVA with Bonferroni post hoc test. #P<0.05, ##P<0.01, and ###P<0.001 for NPFFR2 KO versus WT mice on the same diet; *P<0.05, **P<0.01, and ***P<0.001 for HFD versus STD mice of the same genotype.

Discussion

Anorexigenic peptides are promising tools for the treatment of obesity and related insulin resistance due to their minimal side effects during long-term treatment [25–27]. Our previous studies reported that the peripheral injection of lipidized PrRP31 enables its central anorexigenic effects, and repeated administration of lipidized PrRP31 reveals strong antiobesity features [16,21]. Lipidized PrRP31 not only has anorexigenic and body weight-lowering effects in

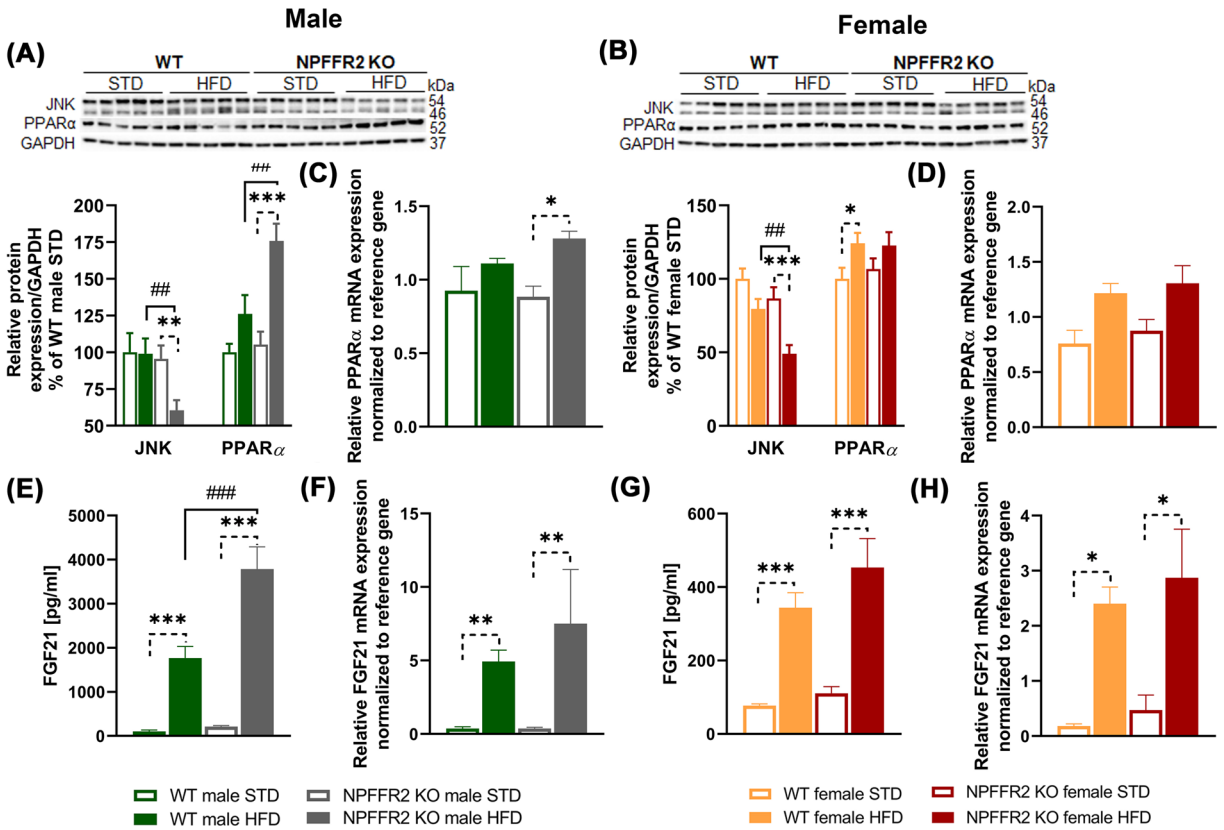

Figure 7. JNK-regulated PPARα-FGF21 axis disruption in NPFFR2 KO males fed a HFD

Western blots for JNK and PPARα in the liver of (**A**) males and (**C**) females. Densitometric quantification of the western blots normalized to GAPDH. mRNA expression of *Pparα* in (**B**) males and (**D**) females. Data are expressed as the mean ± SEM (n=5). FGF21 levels in fasted plasma in (**E**) males and (**G**) females. Data are expressed as the mean ± SEM (n=10). mRNA expression of *Fgf21* in the liver in (**F**) males and (**H**) females. Data are expressed as the mean ± SEM (n=4–5). All data were analyzed by one-way ANOVA with Bonferroni post hoc test. #P<0.05, ##P<0.01, and ###P<0.001 for NPFFR2 KO versus WT mice on the same diet; *P<0.05, **P<0.01, and ***P<0.001 for HFD versus STD mice of the same genotype.

rodent models of obesity but also improves tolerance to glucose in obese Koletsky rats with a mutation in the leptin receptor [28]. PrRP is a promiscuous ligand of two receptors, namely, GPR10 and NPFFR2, and it has a high affinity for NPFFR1 [7]. Our recent study showed that the most potent dual agonists with stabilized N- and C-termini and palmitoylated through the different linkers to Lys^{11} reveal strong antiobesity properties in mouse model of obesity [29]. Therefore, GPR10, NPFFR2, or both may be responsible for the ability of natural PrRP and the lipidized PrRP to reduce body weight and increase glucose tolerance.

The present study was connected to our previous study on GPR10-deficient mice of both sexes fed either a STD or HFD [19] as well as other studies [30,31]. GPR10 gene deletion results in sex-specific changes in lipid metabolism and enhances adipose tissue only in GPR10 KO males but not females, in which the gene expression of proteins regulating lipid metabolism is augmented [19].

Recently, NPFF-deficient mice have been produced and show reduced repetitive and anxiety-like behavior with unchanged energy expenditure, feeding behavior, and body weight [32]. NPFFR2 directly stimulates the hypothalamic–pituitary–adrenal (HPA) axis through the paraventricular nucleus, and deletion of NPFFR2 reduces anxiety-like behavior in response to a single prolonged stress [33,34]. In the present study, although both NPFFR2 KO and WT mice fed a HFD showed reduced tendencies to explore the arena and avoided open regions in the OF, we did not observe anxiety-like behavior caused by NPFFR2 deletion.

In the present study, we did not observe increased adipose tissue mass or increased body weight owing to NPFFR2 deficiency in STD- or HFD-fed mice of both sexes. Surprisingly, HFD-fed NPFFR2 KO males had lower body weight, gWAT weight, scWAT weight, leptin plasma levels, and liver weight compared with their WT controls. By the production of nitric oxide, leptin could directly stimulate lipolysis in adipocytes by an autocrine action on adipocyte leptin

Clinical Science (2023) **137** 847–862
https://doi.org/10.1042/CS20220880

receptors [35,36]. We could conclude that a lower plasma leptin in HFD fed NPFF2 KO males could result in a lower lipolysis, but not at the level of mRNA expression of lipolytic enzymes that did not show genotype-related changes in both scWAT and gWAT. In contrast, Zhang et al. reported that NPFFR2 deficiency does not affect the growth curve of STD-fed mice but instead increases body weight in HFD-fed mice [9]. Moreover, mRNA expression of PrRP did not change in NPFF-/- model by Zhang et al. [9], but our model did not show any difference between genotypes.

The present study clearly demonstrated that NPFFR2 deficiency led to strong glucose intolerance in both STD- and HFD-fed mice of both sexes. Furthermore, NPFFR2 KO mice fed a HFD showed substantially greater glucose excursions than their WT controls.

Recently, Zhang et al. reported that NPFF deficiency improves glucose tolerance without insulin excursions and that HFD-induced glucose intolerance is ameliorated by NPFF deficiency [5]. As NPFFR2 also has another high-affinity ligand, PrRP, it should be taken into account that NPFFR2 may be activated by PrRP in NPFF-deficient mice. In the dorsal vagal complex (DVC), namely, the nucleus of the tractus solitarius and the area postrema, colocalization of PrRP and GPR10 has been reported [37]. Similar to NPFF, NPFFR2 has been found to colocalize in another DVC domain, the subpostrema area [5]. Thus, in the DVC of NPFF-deficient mice, PrRP, another NPFFR2 ligand, may be available to compensate for the absence of NPFF and fulfill the role in glucose metabolic control suggested by Zhang et al. [5]. Severe intolerance to glucose in NPFFR2 KO mice suggested the development of insulin resistance. NPFFR2 KO mice showed worsened glucose intolerance when fed a HFD and displayed a significant decrease in the total protein levels of the PI3K p85 subunit and Akt in the hypothalamus of both sexes and in the liver of females. These results suggested that NPFFR2 deficiency causes dysregulation of central insulin signaling.

Even short-term HFD feeding causes structural and functional changes in the mediobasal hypothalamus, thus affecting caloric intake, energy expenditure, and systemic glucose tolerance [38,39]. Diet-induced obesity has been shown to be associated with a decrease in both leptin and insulin signaling in the hypothalamus [40,41]. Even though NPFFR2 deletion did not alter plasma insulin in fasted animals in the present study, NPFFR2 KO mice displayed imperfect brain PI3K/Akt signaling owing to decreased insulin signaling proteins in the hypothalamus and brainstem, two essential regions regulating energy metabolism, after feeding a HFD for 17 weeks. This finding highlighted the important role of NPFFR2 in the sensitivity to insulin.

The resistance against the development of fatty liver in HFD-fed males, which was even more pronounced in NPFFR2 KO males, led to the determination of PPARα as a positive regulator of fatty acid β-oxidation in peroxisomes and mitochondria. The metabolic stress generated by HFD in the liver relates to hepatic JNK. JNK signaling plays an important role in the regulation of glucose tolerance and TAG accumulation in the liver [42–44]. It has been shown that HFD-fed JNK1 null mice have enhanced insulin sensitivity and attenuated hepatic steatosis [42,43], and HFD-fed mice with liver-specific JNK2 KO show improved glucose tolerance and lowered hepatic insulin resistance [45]. Hepatic JNK activation suppresses *Pparα* gene expression, which promotes fatty liver and insulin resistance [46]. In the present study, we found a significant reduction in JNK in HFD-fed NPFFR2 KO mice of both sexes compared with their respective WT controls. This finding suggested that a decrease in JNK led to increased total PPARα protein in NPFFR2 KO males fed a HFD, resulting in a significantly elevated FGF21 level in fasted plasma. PPARα acts as a transcription factor of the FGF21 hepatokine that then acts as a paracrine hormone in the liver and as a circulating hormone-targeting adipose tissue. In both liver and adipose tissue, FGF21 promotes fatty acid β-oxidation in peroxisomes and mitochondria, thus ultimately acting against lipid deposition in the liver and lower the weight of gWAT and scWAT. The decreased liver metabolic stress in NPFFR2 KO males cannot be attributed to NPFFR2 deficiency in the liver as WT mice do not express *Npffr2* in the liver [8]. In contrast, adipose tissue, which generally affects liver metabolism to a great extent, has high levels of *Npffr2* mRNA. However, NPFFR2 deletion had only a few effects on adipose tissue.

Decreased mRNA expression of the proinflammatory cytokine, *Tnfα*, in BAT and eWAT of HFD-fed NPFFR2 KO males is not related to their lower body weight [47]. Adipose tissue lipolysis is decreased in NPFFR2 KO females, but not in males, owing their reduced mRNA expression of *Adra3β* in both the gWAT and scWAT [48]. In rodents, *Adra3β* controls BAT thermogenesis and has a protective effect against obesity development. Similar to *Adra3β*, *adiponectin* and *Pparγ* mRNA expression was lowered only in females. As both *Adra3β* and *Pparγ* support lipolysis, lipolysis in adipose tissue was attenuated by NPFFR2 deficiency only in females. However, in males, adipose tissue lipolysis was enhanced by FGF21 action.

In conclusion, metabolic phenotyping in the present study showed that deletion of NPFFR2 did not alter normal behavior or pain perception. Both male and female NPFFR2 KO mice fed a STD revealed a lean phenotype, but HFD-fed NPFFR2 KO males had lower body, gWAT, scWAT, and liver weights as well as lower plasma leptin levels compared with their WT controls. In contrast, deletion of the NPFFR2 gene resulted in strong glucose intolerance in both males and females fed a HFD and was accompanied by disturbed brain insulin signaling. In HFD-fed NPFFR2

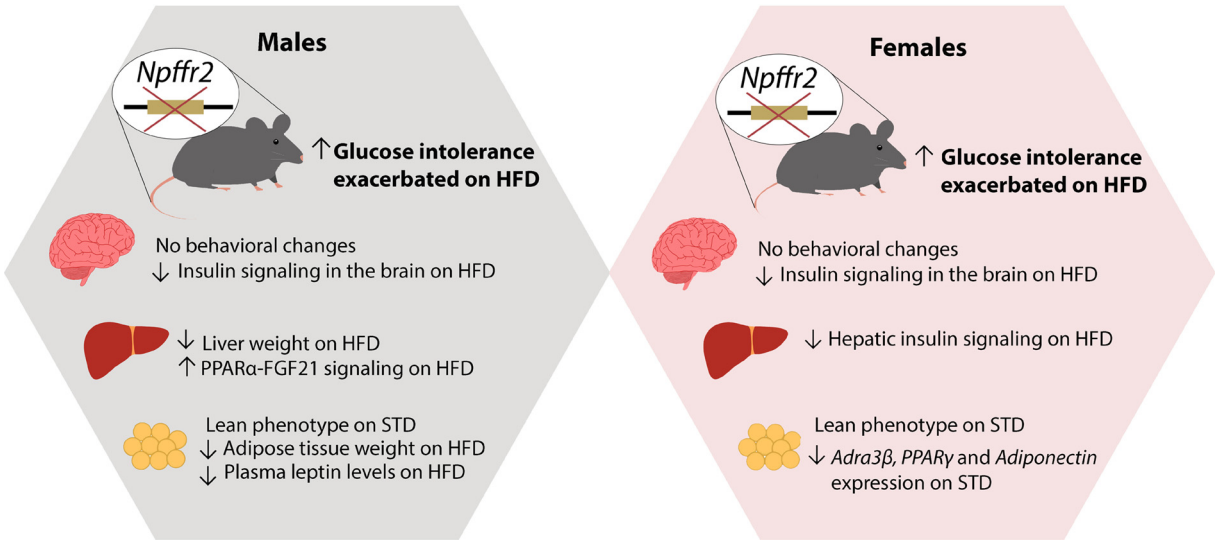

Figure 8. Overview of changes as a consequence of NPFFR2 gene deletion

KO males, the hepatic JNK-regulated PPAR-FGF21 axis was up-regulated, probably to compensate for metabolic stress. The most significant changes are summarized in Figure 8.

Clinical perspectives

- Lipidized PrRP analogs showed dual GPR10-NPFFR2 agonist properties, but the mechanism by which PrRPs analogs control food intake and glucose homeostasis remains unclear; hence, NPFFR2 deletion may provide insight into the antidiabetic mechanisms of action of PrRPs analogs.
- The present study demonstrated augmented glucose intolerance and disrupted central insulin signaling in the absence of NPFFR2.
- Targeting NPFFR2 signaling may provide a new approach for the treatment of obesity and type 2 diabetes.

Data Availability

All data are included in the manuscript.

Competing Interests

The authors declare that there are no competing interests associated with the manuscript.

Funding

This research was supported by the Czech Science Foundation [grant numbers 21-03691S and RVO:61388963 and RVO:67985823] of Czech Academy of Sciences. This work was also supported by the project National Institute for Research on Cardiovascular Diseases Related to Metabolic Diseases of Diabetes and Obesity (Programme EXCELES, ID Project No. LX22NP05104) – Funded by the European Union – Next Generation EU. Novo Nordisk A/S supported the study with research funding. The results were obtained using research infrastructure of Czech center of phenogenomics supported by the projects LM2018126 and CZ.1.05/2.1.00/19.0395 a CZ.1.05/1.1.00/02.0109 of Czech Ministery of Education.

CRediT Author Contribution

Alena Karnošová: Conceptualization, Data curation, Formal Analysis, Investigation, Methodology, Writing—original draft. **Veronika Strnadová:** Conceptualization, Data curation, Formal Analysis, Supervision, Investigation, Methodology,

Clinical Science (2023) **137** 847–862
https://doi.org/10.1042/CS20220880

Writing—original draft. **Blanka—Železná:** Conceptualization, Validation, Investigation, Writing—review & editing. **Jaroslav Kuneš:** Data curation, Supervision, Investigation, Writing—review & editing. **Petr Kašpárek:** Data curation, Methodology, Writing—original draft. **Lenka Maletínská:** Conceptualization, Resources, Supervision, Investigation, Writing—review & editing.

Acknowledgements

The authors thank Hedvika Vysušilová (Institute of Organic Chemistry and Biochemistry of the Czech Academy of Sciences, Prague, Czech Republic) for her excellent technical assistance and animal handling. Miloslava Čechová (IKEM) for mRNA analysis.

Abbreviations

AUC, area under the curve; BAT, brown adipose tissue; b2M, beta-2-microglobulin; CNS, central nervous system; DVC, dorsal vagal complex; EPM, elevated plus maze; FFA, free fatty acid; FGF21, fibroblast growth factor 21; GAPDH, glyceraldehyde 3-phosphate dehydrogenase; gRNA, guide RNA; gWAT, gonadal white adipose tissue; HPA, hypothalamic–pituitary–adrenal; HFD, high-fat diet; HP, hot plate; JNK, c-Jun NH_2-terminal kinase; KO, knockout; NPFF, neuropeptide FF; NPFFR2, neuropeptide FF receptor 2; NPY, neuropeptide Y; OF, open field; OGTT, oral glucose tolerance test; PDK, phosphoinositide-dependent protein kinase; PI3K, phosphoinositide 3-kinase; PrRP, prolactin-releasing peptide; scWAT, subcutaneous white adipose tissue; STD, standard diet; TAG, triacylglycerol; UCP1, uncoupling protein-1; WT, wild-type.

References

1 Elhabazi, K., Humbert, J.P., Bertin, I., Schmitt, M., Bihel, F., Bourguignon, J.J. et al. (2013) Endogenous mammalian RF-amide peptides, including PrRP, kisspeptin and 26RFa, modulate nociception and morphine analgesia via NPFF receptors. *Neuropharmacology* **75**, 164–171, https://doi.org/10.1016/j.neuropharm.2013.07.012

2 Murase, T., Arima, H., Kondo, K. and Oiso, Y. (1996) Neuropeptide FF reduces food intake in rats. *Peptides* **17**, 353–354, https://doi.org/10.1016/0196-9781(95)02137-X

3 Sunter, D., Hewson, A.K., Lynam, S. and Dickson, S.L. (2001) Intracerebroventricular injection of neuropeptide FF, an opioid modulating neuropeptide, acutely reduces food intake and stimulates water intake in the rat. *Neurosci. Lett.* **313**, 145–148, https://doi.org/10.1016/S0304-3940(01)02267-4

4 Cline, M.A., Nandar, W. and Rogers, J.O. (2007) Central neuropeptide FF reduces feed consumption and affects hypothalamic chemistry in chicks. *Neuropeptides* **41**, 433–439, https://doi.org/10.1016/j.npep.2007.08.003

5 Zhang, L., Koller, J., Gopalasingam, G., Qi, Y. and Herzog, H. (2022) Central NPFF signalling is critical in the regulation of glucose homeostasis. *Mol. Metab.* **62**, 101525, https://doi.org/10.1016/j.molmet.2022.101525

6 Lefrere, I., De Coppet, P., Camelin, J.C., Le Lay, S., Mercier, N., Elshourbagy, N. et al. (2002) Neuropeptide AF and FF modulation of adipocyte metabolism. Primary insights from functional genomics and effects on beta-adrenergic responsiveness. *J. Biol. Chem.* **277**, 39169–39178

7 Karnosova, A., Strnadova, V., Hola, L., Zelezna, B., Kunes, J. and Maletinska, L. (2021) Palmitoylation of prolactin-releasing peptide increased affinity for and activation of the GPR10, NPFF-R2 and NPFF-R1 receptors: in vitro study. *Int. J. Mol. Sci.* **22**, 8904–24, https://doi.org/10.3390/ijms22168904

8 Bonini, J.A., Jones, K.A., Adham, N., Forray, C., Artymyshyn, R., Durkin, M.M. et al. (2000) Identification and characterization of two G protein-coupled receptors for neuropeptide FF. *J. Biol. Chem.* **275**, 39324–39331, https://doi.org/10.1074/jbc.M004385200

9 Zhang, L., Ip, C.K., Lee, I.J., Qi, Y., Reed, F., Karl, T. et al. (2018) Diet-induced adaptive thermogenesis requires neuropeptide FF receptor-2 signalling. *Nat. Commun.* **9**, 4722, https://doi.org/10.1038/s41467-018-06462-0

10 Yi, M., Li, H., Wu, Z., Yan, J., Liu, Q., Ou, C. et al. (2018) A promising therapeutic target for metabolic diseases: neuropeptide Y receptors in humans. *Cell. Physiol. Biochem.* **45**, 88–107, https://doi.org/10.1159/000486225

11 Gouardères, C., Quelven, I., Mollereau, C., Mazarguil, H., Rice, S.Q. and Zajac, J.M. (2002) Quantitative autoradiographic distribution of NPFF1 neuropeptide FF receptor in the rat brain and comparison with NPFF2 receptor by using [125I]YVP and [(125I]EYF as selective radioligands. *Neuroscience* **115**, 349–361, https://doi.org/10.1016/S0306-4522(02)00419-0

12 Goncharuk, V. and Jhamandas, J.H. (2008) Neuropeptide FF2 receptor distribution in the human brain. An immunohistochemical study. *Peptides* **29**, 1544–1553, https://doi.org/10.1016/j.peptides.2008.05.004

13 Gouardères, C., Puget, A. and Zajac, J.M. (2004) Detailed distribution of neuropeptide FF receptors (NPFF1 and NPFF2) in the rat, mouse, octodon, rabbit, guinea pig, and marmoset monkey brains: a comparative autoradiographic study. *Synapse* **51**, 249–269, https://doi.org/10.1002/syn.10305

14 Liu, Q., Guan, X.M., Martin, W.J., McDonald, T.P., Clements, M.K., Jiang, Q. et al. (2001) Identification and characterization of novel mammalian neuropeptide FF-like peptides that attenuate morphine-induced antinociception. *J. Biol. Chem.* **276**, 36961–36969, https://doi.org/10.1074/jbc.M105308200

15 Waqas, S.F.H., Hoang, A.C., Lin, Y.T., Ampem, G., Azegrouz, H., Balogh, L. et al. (2017) Neuropeptide FF increases M2 activation and self-renewal of adipose tissue macrophages. *J. Clin. Invest.* **127**, 2842–2854, https://doi.org/10.1172/JCI90152

16 Prazienkova, V., Holubova, M., Pelantova, H., Buganova, M., Pirnik, Z., Mikulaskova, B. et al. (2017) Impact of novel palmitoylated prolactin-releasing peptide analogs on metabolic changes in mice with diet-induced obesity. *PloS ONE* **12**, e0183449, https://doi.org/10.1371/journal.pone.0183449

17 Maletinska, L., Nagelova, V., Ticha, A., Zemenova, J., Pirnik, Z., Holubova, M. et al. (2015) Novel lipidized analogs of prolactin-releasing peptide have prolonged half-lives and exert anti-obesity effects after peripheral administration. *Int. J. Obesity* **39**, 986–993, https://doi.org/10.1038/ijo.2015.28

18 Kunes, J., Prazienkova, V., Popelova, A., Mikulaskova, B., Zemenova, J. and Maletinska, L. (2016) Prolactin-releasing peptide: a new tool for obesity treatment. *J. Endocrinol.* **230**, R51–R58, https://doi.org/10.1530/JOE-16-0046

19 Prazienkova, V., Funda, J., Pirnik, Z., Karnosova, A., Hruba, L., Korinkova, L. et al. (2021) GPR10 gene deletion in mice increases basal neuronal activity, disturbs insulin sensitivity and alters lipid homeostasis. *Gene* **774**, 145427, https://doi.org/10.1016/j.gene.2021.145427
20 Jenickova, I., Kasparek, P., Petrezselyova, S., Elias, J., Prochazka, J., Kopkanova, J. et al. (2021) Efficient allele conversion in mouse zygotes and primary cells based on electroporation of Cre protein. *Methods* **191**, 87–94, https://doi.org/10.1016/j.ymeth.2020.07.005
21 Maletinska, L., Nagelova, V., Ticha, A., Zemenova, J., Pirnik, Z., Holubova, M. et al. (2015) Novel lipidized analogs of prolactin-releasing peptide have prolonged half-lives and exert anti-obesity effects after peripheral administration. *Int. J. Obes. (Lond.)* **39**, 986–993, https://doi.org/10.1038/ijo.2015.28
22 Blechova, M., Nagelova, V., Zakova, L., Demianova, Z., Zelezna, B. and Maletinska, L. (2013) New analogs of the CART peptide with anorexigenic potency: the importance of individual disulfide bridges. *Peptides* **39**, 138–144, https://doi.org/10.1016/j.peptides.2012.09.033
23 Maletinska, L., Matyskova, R., Maixnerova, J., Sykora, D., Pychova, M., Spolcova, A. et al. (2011) The peptidic GHS-R antagonist [D-Lys(3)]GHRP-6 markedly improves adiposity and related metabolic abnormalities in a mouse model of postmenopausal obesity. *Mol. Cell. Endocrinol.* **343**, 55–62, https://doi.org/10.1016/j.mce.2011.06.006
24 Spolcova, A., Mikulaskova, B., Holubova, M., Nagelova, V., Pirnik, Z., Zemenova, J. et al. (2015) Anorexigenic lipopeptides ameliorate central insulin signaling and attenuate tau phosphorylation in hippocampi of mice with monosodium glutamate-induced obesity. *J. Alzheimers Dis.* **45**, 823–835, https://doi.org/10.3233/JAD-143150
25 Arch, J.R. (2015) Horizons in the pharmacotherapy of obesity. *Curr. Obes. Rep.* **4**, 451–459, https://doi.org/10.1007/s13679-015-0177-4
26 Patel, D. (2015) Pharmacotherapy for the management of obesity. *Metabolism* **64**, 1376–1385, https://doi.org/10.1016/j.metabol.2015.08.001
27 Bray, G.A., Frühbeck, G., Ryan, D.H. and Wilding, J.P.H. (2016) Management of obesity. *Lancet North Am. Ed.* **387**, 1947–1956, https://doi.org/10.1016/S0140-6736(16)00271-3
28 Mikulaskova, B., Holubova, M., Prazienkova, V., Zemenova, J., Hruba, L., Haluzik, M. et al. (2018) Lipidized prolactin-releasing peptide improved glucose tolerance in metabolic syndrome: Koletsky and spontaneously hypertensive rat study. *Nutr. Diab.* **8**, 5, https://doi.org/10.1038/s41387-017-0015-8
29 Strnadova, V., Karnosova, A., Blechova, M., Neprasova, B., Hola, L., Nemcova, A. et al. (2023) Search for lipidized PrRP analogs with strong anorexigenic effect: in vitro and in vivo studies. *Neuropeptides* **98**, 102319, https://doi.org/10.1016/j.npep.2022.102319
30 Gu, W., Geddes, B.J., Zhang, C., Foley, K.P. and Stricker-Krongrad, A. (2004) The prolactin-releasing peptide receptor (GPR10) regulates body weight homeostasis in mice. *J. Mol. Neurosci.* **22**, 93–103, https://doi.org/10.1385/JMN:22:1-2:93
31 Bjursell, M., Lenneras, M., Goransson, M., Elmgren, A. and Bohlooly, Y.M. (2007) GPR10 deficiency in mice results in altered energy expenditure and obesity. *Biochem. Biophys. Res. Commun.* **363**, 633–638, https://doi.org/10.1016/j.bbrc.2007.09.016
32 Zhang, L., Koller, J., Ip, C.K., Gopalasingam, G., Bajaj, N., Lee, N.J. et al. (2021) Lack of neuropeptide FF signalling in mice leads to reduced repetitive behavior, altered drinking behavior, and fuel type selection. *FASEB J.* **35**, e21980, https://doi.org/10.1096/fj.202100703R
33 Lin, Y.T., Yu, Y.L., Hong, W.C., Yeh, T.S., Chen, T.C. and Chen, J.C. (2017) NPFFR2 activates the HPA axis and induces anxiogenic effects in rodents. *Int. J. Mol. Sci.* **18**, 1018–23, https://doi.org/10.3390/ijms18081810
34 Lin, Y.T., Huang, Y.L., Tsai, S.C. and Chen, J.C. (2020) Ablation of NPFFR2 in mice reduces response to single prolonged stress model. *Cells* **9**, 2479–92, https://doi.org/10.3390/cells9112479
35 Fruhbeck, G. and Gomez-Ambrosi, J. (2001) Modulation of the leptin-induced white adipose tissue lipolysis by nitric oxide. *Cell. Signal.* **13**, 827–833, https://doi.org/10.1016/S0898-6568(01)00211-X
36 Fruhbeck, G., Gomez-Ambrosi, J. and Salvador, J. (2001) Leptin-induced lipolysis opposes the tonic inhibition of endogenous adenosine in white adipocytes. *FASEB J.* **15**, 333–340, https://doi.org/10.1096/fj.00-0249com
37 Dodd, G.T. and Luckman, S.M. (2013) Physiological roles of GPR10 and PrRP signaling. *Front Endocrinol. (Lausanne)* **4**, 20, https://doi.org/10.3389/fendo.2013.00020
38 Engel, D.F. and Velloso, L.A. (2022) The timeline of neuronal and glial alterations in experimental obesity. *Neuropharmacology* **208**, 108983, https://doi.org/10.1016/j.neuropharm.2022.108983
39 Ullah, R., Rauf, N., Nabi, G., Yi, S., Yu-Dong, Z. and Fu, J. (2021) Mechanistic insight into high-fat diet-induced metabolic inflammation in the arcuate nucleus of the hypothalamus. *Biomed. Pharmacother.* **142**, 112012, https://doi.org/10.1016/j.biopha.2021.112012
40 Balland, E., Chen, W., Dodd, G.T., Conductier, G., Coppari, R., Tiganis, T. et al. (2019) Leptin signaling in the arcuate nucleus reduces insulin's capacity to suppress hepatic glucose production in obese mice. *Cell Rep.* **26**, 346–355, e343, https://doi.org/10.1016/j.celrep.2018.12.061
41 de Carvalho, F.P., Moretto, T.L., Benfato, I.D., Barthichoto, M., Ferreira, S.M., Costa-Junior, J.M. et al. (2018) Central and peripheral effects of physical exercise without weight reduction in obese and lean mice. *Biosci. Rep.* **38**, BSR20171033, https://doi.org/10.1042/BSR20171033
42 Tuncman, G., Hirosumi, J., Solinas, G., Chang, L., Karin, M. and Hotamisligil, G.S. (2006) Functional in vivo interactions between JNK1 and JNK2 isoforms in obesity and insulin resistance. *Proc. Natl. Acad. Sci. U.S.A.* **103**, 10741–10746, https://doi.org/10.1073/pnas.0603509103
43 Schattenberg, J.M., Singh, R., Wang, Y., Lefkowitch, J.H., Rigoli, R.M., Scherer, P.E. et al. (2006) JNK1 but not JNK2 promotes the development of steatohepatitis in mice. *Hepatology* **43**, 163–172, https://doi.org/10.1002/hep.20999
44 Singh, R., Wang, Y., Xiang, Y., Tanaka, K.E., Gaarde, W.A. and Czaja, M.J. (2009) Differential effects of JNK1 and JNK2 inhibition on murine steatohepatitis and insulin resistance. *Hepatology* **49**, 87–96, https://doi.org/10.1002/hep.22578
45 Vernia, S., Cavanagh-Kyros, J., Garcia-Haro, L., Sabio, G., Barrett, T., Jung, D.Y. et al. (2014) The PPARalpha-FGF21 hormone axis contributes to metabolic regulation by the hepatic JNK signaling pathway. *Cell Metab.* **20**, 512–525, https://doi.org/10.1016/j.cmet.2014.06.010
46 Solinas, G. and Becattini, B. (2017) JNK at the crossroad of obesity, insulin resistance, and cell stress response. *Mol. Metab.* **6**, 174–184, https://doi.org/10.1016/j.molmet.2016.12.001
47 Tzanavari, T., Giannogonas, P. and Karalis, K.P. (2010) TNF-alpha and obesity. *Curr. Dir. Autoimmun.* **11**, 145–156, https://doi.org/10.1159/000289203

Clinical Science (2023) **137** 847–862
https://doi.org/10.1042/CS20220880

48 Valentine, J.M., Ahmadian, M., Keinan, O., Abu-Odeh, M., Zhao, P., Zhou, X. et al. (2022) beta3-Adrenergic receptor downregulation leads to adipocyte catecholamine resistance in obesity. *J. Clin. Invest.* **132**, e153357, https://doi.org/10.1172/JCI153357

Supplementary data

Supplementary Table 1. List of tested genes of interest in different tissues

Gene	BAT	scWAT	gWAT	liver
acetyl-CoA carboxylase 1 (*Acaca*)		x	x	x
adiponectin		x	x	
adrenoreceptor 3β (*Adr3b*)	x	x	x	
3-hydroxybutyrate dehydrogenase 1 (Bdh1)				x
carbohydrate-responsive element-binding protein (*Chrebp*)		x	x	
carnitine palmitoyltransferase 1A (*Cpt1α*)		x	x	x
fatty acid synthase (*Fasn*)		x	x	
fibroblast growth factor 21 (*Fgf21*)				x
glucose transporter type 4 (*Glut4*)		x	x	
glycogen synthase kinase-3 β (*Gsk3β*)				x
3-hydroxy-3-methylglutaryl-CoA lyase (*Hmgcl*)				x
3-hydroxy-3-methylglutaryl-CoA synthase 1 (*Hmgcs1*)				x
insulin receptor substrate 1 (*Irs1*)		x	x	x
insulin receptor substrate 2 (*Irs2*)		x	x	x
lipase E, hormone sensitive type (*Lipe*)		x	x	
patatin like phospholipase domain containing 2 (*Pnpla2*)		x	x	
peroxisome proliferator-activated receptor alpha (*Pparα*)				x
peroxisome proliferator-activated receptor gamma (*Pparγ*)		x	x	
peroxisome proliferator activator receptor gamma coactivator 1 alpha (*Pparγc1a*)	x	x	x	x
PR/SET domain 16 (*Prdm16*)	x			
stearoyl-CoA desaturase 1 (*Scd1*)		x	x	x
sterol regulatory element-binding transcription factor 1 (*Srebp1*)		x	x	
uncoupling protein 1 (*Ucp1*)	x			
vascular endothelial growth factor alpha (*Vegfα*)	x			
tumor necrosis factor alpha (*TNFα*)	x	x	x	

Supplementary Table 2. List of used primary antibodies

Abbreviation	Antibody	MW kDa	Dilution	Provider
p-Akt S473	Phospho-Akt (Ser473) (D9E) XP® Rabbit mAb #4060	60	1:1000	Cell Signaling Technology
Akt	Akt (pan) (C67E7) Rabbit mAb #4691	60	1:1000	Cell Signaling Technology
p-AS160 S588	Phospho-AS160 (Ser588) (D8E4) Rabbit mAb #8730	160	1:1000	Cell Signaling Technology
AS160	AS160 (C69A7) Rabbit mAb #2670	160	1:1000	Cell Signaling Technology
GAPDH	GAPDH (D4C6R) Mouse mAb #97166	37	1:1000	Cell Signaling Technology
JNK	SAPK/JNK Antibody Rabbit #9252	46, 54	1:1000	Cell Signaling Technology
p-PDK	Phospho-PDK1 (Ser241) (C49H2) Rabbit mAb #3438	58-68	1:0000	Cell Signaling Technology
PDK	PDK1 Antibody Rabbit Ab #3062	58-68	1:0000	Cell Signaling Technology
PI3K p85	PI3 Kinase p85 (19H8) Rabbit mAb #4257	85	1:1000	Cell Signaling Technology
PI3K p110α	PI3 Kinase p110α (C73F8) Rabbit mAb #4249	110	1:1000	Cell Signaling Technology
PPARα	PPAα Polyclonal Rabbit Ab #PA1-822A	52	1:1000	Thermo Fisher Scientific Inc.

Supplementary Table 3. Morphometric analysis in NPFFR2 KO and WT mice at 26 weeks and plasma metabolic profile at 24 weeks

group	BW [g]	BAT [g]	scWAT [g]	gWAT [g]	liver [g]	TAG	FFA	cholesterol	leptin
WT male STD	29.96 ± 0.32	0.11 ± 0.01	0.24 ± 0.02	0.40 ± 0.02	1.33 ± 0.05	0.45 ± 0.02	0.73 ± 0.10	1.95 ± 0.12	1.85 ± 0.30
NPFFR2 KO male STD	30.34 ± 0.63	0.14 ± 0.01	0.30 ± 0.02	0.47 ± 0.06	1.38 ± 0.05	0.43 ± 0.03	0.57 ± 0.06	1.89 ± 0.12	2.92 ± 0.78
WT male HFD	51.33 ± 0.43 ###	0.33 ± 0.02 ###	2.17 ± 0.12 ###	2.30 ± 0.12 ###	1.79 ± 0.05 ###	0.54 ± 0.04	0.60 ± 0.04	3.98 ± 0.07 ###	44.85 ± 1.61 ###
NPFFR2 KO male HFD	44.65 ± 0.77 ###, ***	0.35 ± 0.03 ###	1.39 ± 0.10 ###, ***	1.87 ± 0.06 ###, ***	1.51 ± 0.08 **	0.55 ± 0.04 #	0.61 ± 0.06	3.87 ± 0.18 ###	30.14 ± 1.84 ###, ***
WT female STD	24.55 ± 0.19	0.08 ± 0.01	0.18 ± 0.02	0.22 ± 0.03	1.10 ± 0.01	0.45 ± 0.03	0.47 ± 0.06	3.36 ± 0.21	1.11 ± 0.09
NPFFR2 KO female STD	24.34 ± 0.19	0.09 ± 0.01	0.25 ± 0.03	0.30 ± 0.03	1.02 ± 0.03	0.35 ± 0.01 *	0.44 ± 0.04	2.17 ± 0.18 **	2.55 ± 0.52
WT female HFD	42.44 ± 1.18 ###	0.21 ± 0.02 ###	1.98 ± 0.16 ###	2.99 ± 0.19 ###	1.28 ± 0.07	0.58 ± 0.02 ##	0.39 ± 0.03	5.49 ± 0.23 ###	44.12 ± 3.59 ###
NPFFR2 KO female HFD	45.55 ± 1.22 ###	0.26 ± 0.02 ###	2.15 ± 0.17 ###	3.27 ± 0.18 ###	1.46 ± 0.10 ###	0.51 ± 0.04 ###	0.38 ± 0.04	6.14 ± 0.28 ###	51.00 ± 3.89 ###

A morphometric analysis was performed on NPFFR2 KO and WT mice at the end of the experiment, which took place at 26 weeks of age. Additionally, a plasma metabolic profile was assessed at 24 weeks of age. Data are expressed as mean ± SEM (n = 8-10), as determined by One-way ANOVA with Bonferroni post hoc test. Significance is * $p < 0.05$, ** $p < 0.01$, *** $p < 0.001$ NPFFR2 KO vs WT mice on the same diet, # $p < 0.05$, ## $p < 0.01$, ### $p < 0.001$ HFD vs STD of the same genotype.Body weight (BW), interscapular brown adipose tissue (BAT), subcutaneous white adipose tissue (scWAT), gonadal white adipose tissue (gWAT), triglycerides (TAG), free fatty acids (FFA).

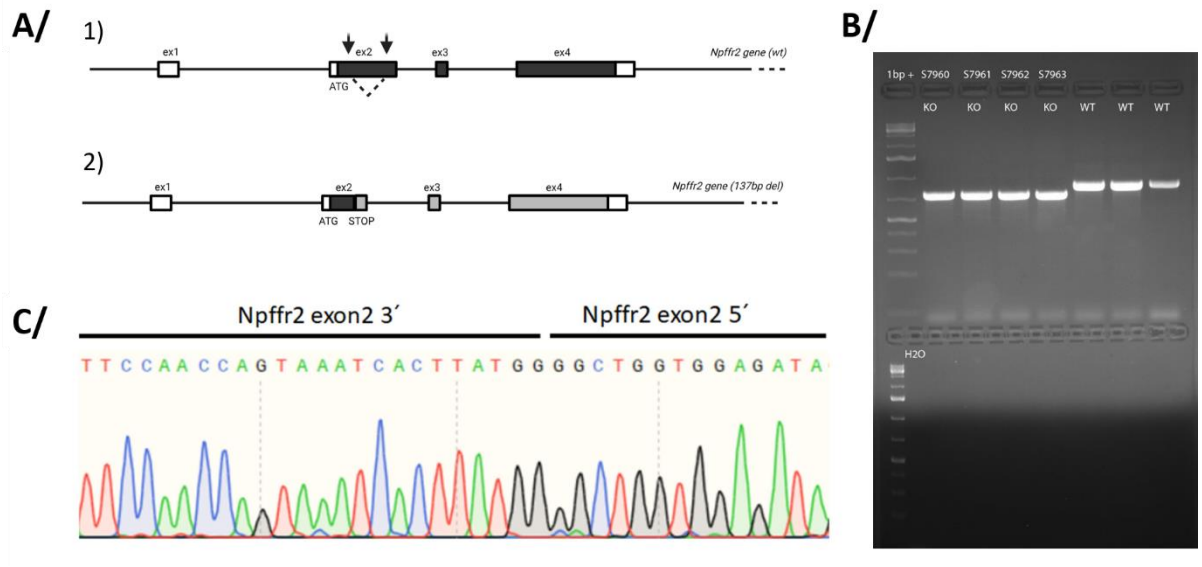

Supplementary Figure 1. Deletion in Npffr2 coding sequence

Schematic representation of the Npffr2 gene targeting strategy (**A**). The wild-type mouse Npffr2 gene locus. Intronic regions are represented as lines, protein-coding exons as black boxes, and untranslated regions as white boxes. The gRNA target sites are marked with black arrows (**1**). Schematics of Npffr2 gene structure after CRISPR-mediated gene targeting in the selected founder line. A 137 bp deletion within exon 2 of Npffr2 leads to a frameshift and generation of a premature STOP codon located in exon 2. This rearrangement results in the elimination of the vast majority of the Npffr2 protein-coding sequence (grey box) (**2**). Gel showing deletion in G1 animals S7960, 61, 62 and 63 and WT animals at 137bp using primers Npffr2-F and R (**B**).Sanger sequencing of the CRISPR target site performed in G1 mouse derived from the founder carrying 137 bp deletion in exon2 of *Npffr2* gene (**C**).

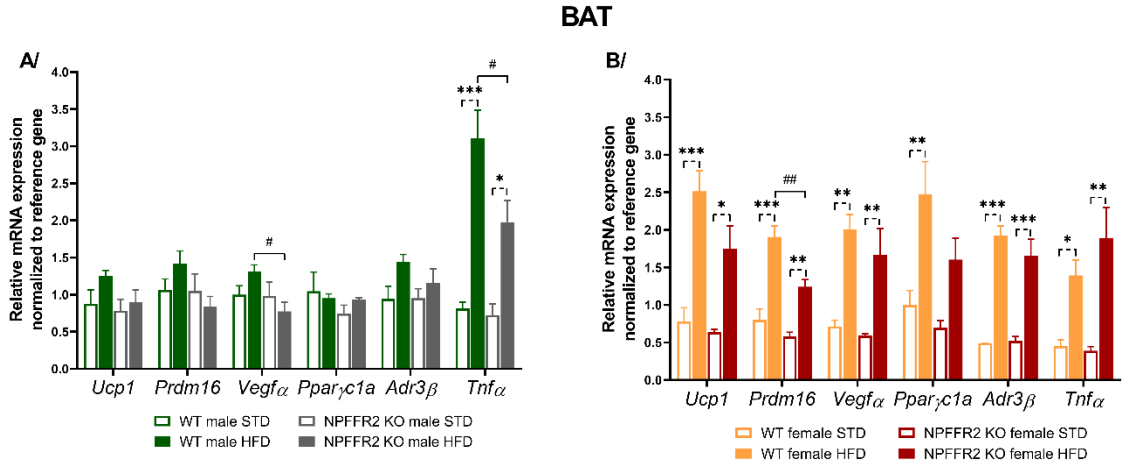

Supplementary Figure 2. Changes in the mRNA expression in the BAT of NPFFR2 KO and WT mice

mRNA expression of *Ucp1*, *Prdm16*, *Vegfα, Pparγc1a, Adr3β*, and *Tnfα* in the BAT of males (**A**)and females (**B**). Data are expressed as the mean ± SEM (n = 5). Significance was determined by one-way ANOVA with Bonferroni post hoc test. * $p < 0.05$, ** $p < 0.01$, and *** $p < 0.001$ for HFD vs. STD mice of the same genotype; # $p < 0.05$ and ## $p < 0.01$ for NPFFR2 KO vs. WT mice on the same diet.

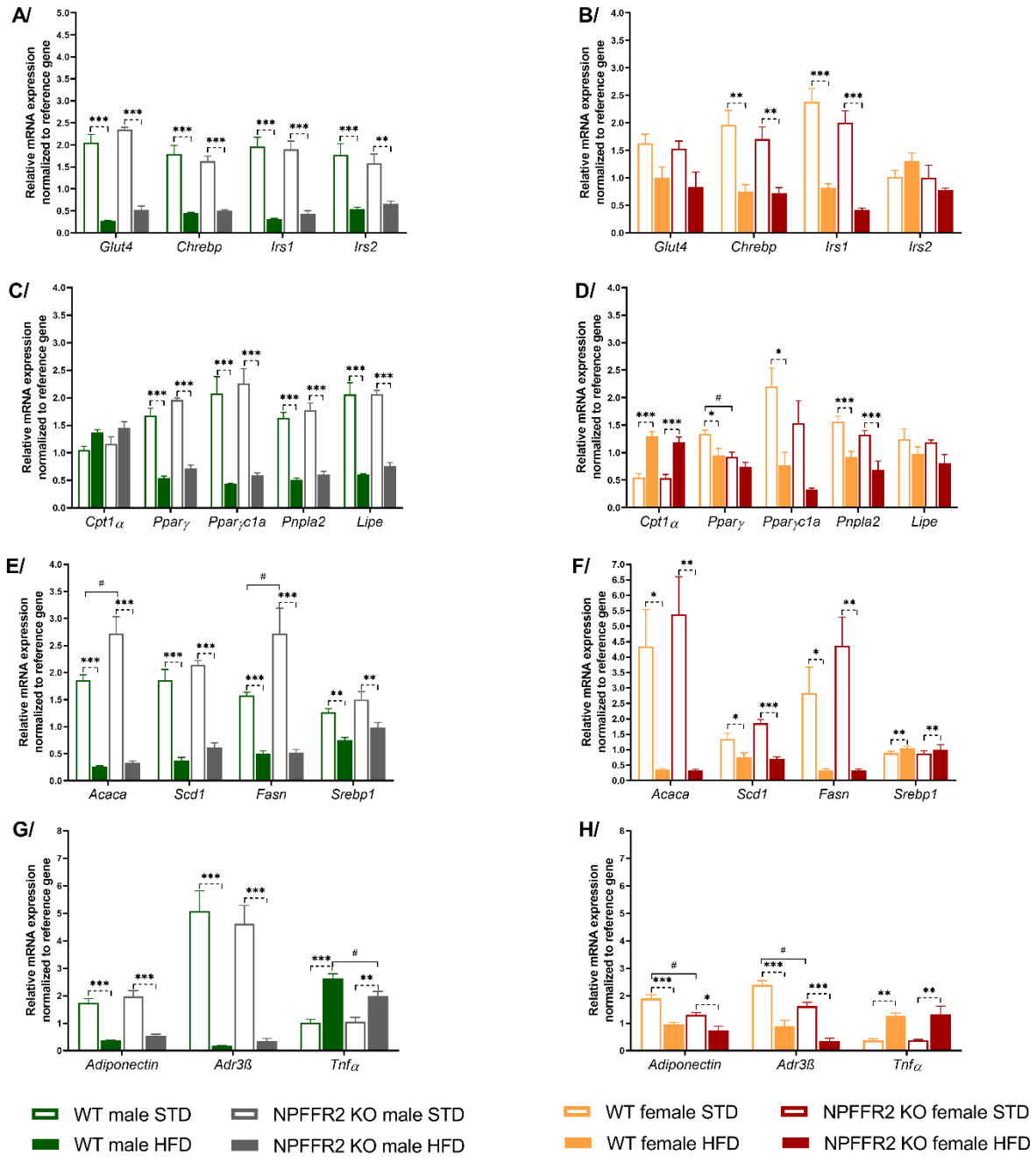

Supplementary Figure 3. Changes in mRNA expression in the gWAT of NPFFR2 KO and WT mice

mRNA expression of genes involved in glucose metabolism in the gWAT in (**A**)males and (**B**) females. mRNA expression of genes involved in lipid metabolism in the gWAT in (**C, E**)males and (**D, F**) females. mRNA expression of *adiponectin*, *Adr3β*, and *Tnfα* in (**G**)males and (**H**) females. Data are expressed as the mean ± SEM (n = 4–5). Significance was determined by one-way ANOVA with Bonferroni post hoc test. * $p < 0.05$, ** $p < 0.01$, and *** $p < 0.001$ for HFD vs. STD mice of the same genotype; # $p < 0.05$ for NPFFR2 KO vs. WT mice on the same diet.

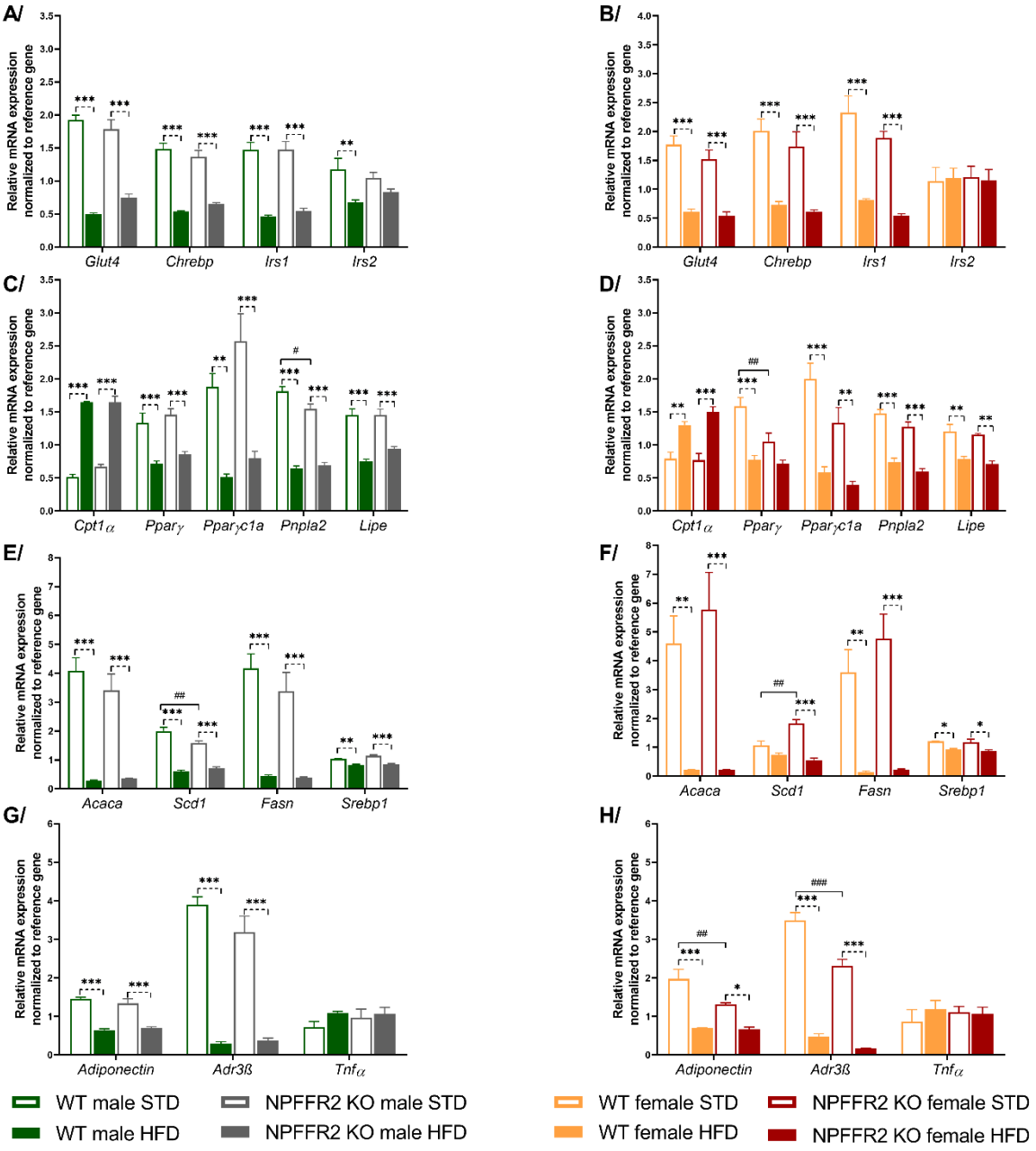

Supplementary Figure 4. Changes in the mRNA expression in the scWAT of NPFFR2 KO and WT mice

mRNA expression of genes involved in glucose metabolism in the scWAT in (**A**)males and (**B**) females. mRNA expression of genes involved in lipid metabolism in the scWAT in (**C, E**)males and (**D, F**) females. mRNA expression of *adiponectin*, *Adr3β*,and *Tnfα* in the scWAT in (**G**)males and (**H**) females. Data are expressed as the mean ± SEM (n = 4–5). Significance was determined by one-way ANOVA with Bonferroni post hoc test. * $p < 0.05$, ** $p < 0.01$, and *** $p < 0.001$ for HFD vs. STD mice of the same genotype; # $p < 0.05$, ## $p < 0.01$, and ### $p < 0.001$ for NPFFR2 KO vs. WT mice on the same diet.

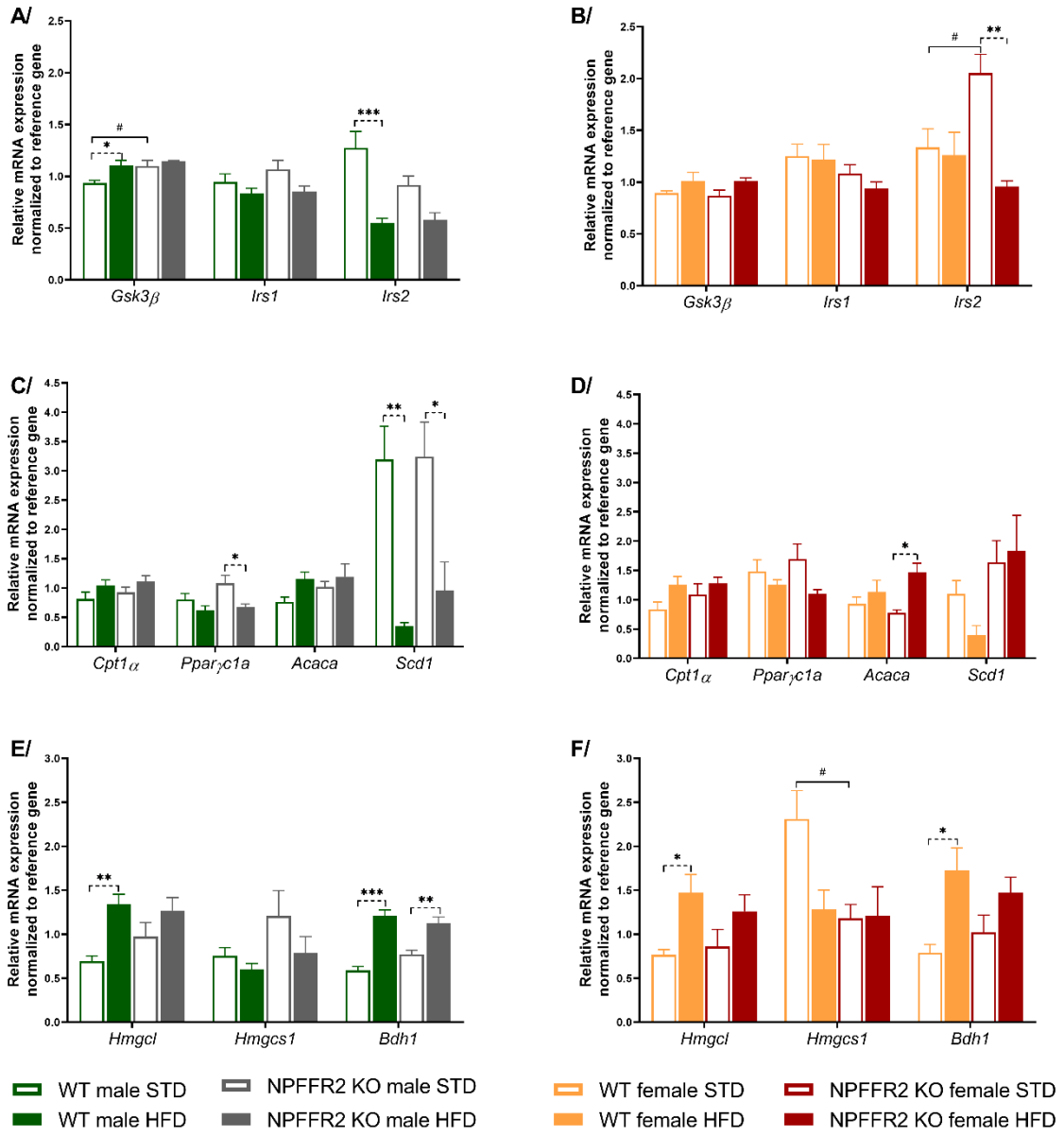

Supplementary Figure 5. Changes in mRNA expression in the livers of NPFFR2 KO and WT mice

mRNA expression of genes involved in glucose metabolism in the liver in (**A**)males and (**B**) females. mRNA expression of genes involved in lipid metabolism in the liver in (**C**)males and (**D**) females. mRNA expression of genes involved in ketogenesis in the liver in (**E**) males and (**F**) females. mRNA expression of *Fgf21* in the liver in (**G**)males and (**H**) females. Data are expressed as the mean ± SEM (n = 5). Significance was determined by one-way ANOVA with Bonferroni post hoc test. * $p < 0.05$, ** $p < 0.01$, and *** $p < 0.001$ for HFD vs. STD mice of the same genotype; # $p < 0.05$ for NPFFR2 KO vs. WT mice on the same diet.

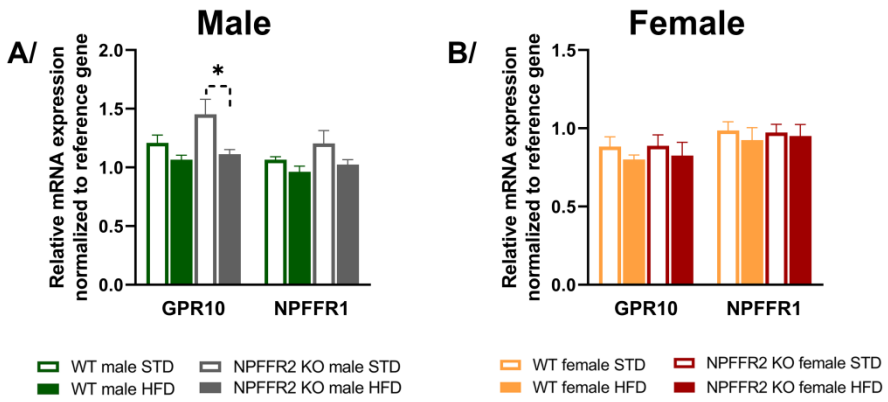

Supplementary Figure 6. Changes in mRNA expression in the hypothalamus of NPFFR2 KO and WT mice. mRNA expression of genes for GPR10 and NPFFR1 in (**A**)males and (**B**) females. Data are expressed as the mean ± SEM (n = 5). Significance was determined by one-way ANOVA with Bonferroni post hoc test. * $p < 0.05$ for HFD vs. STD mice of the same genotype.

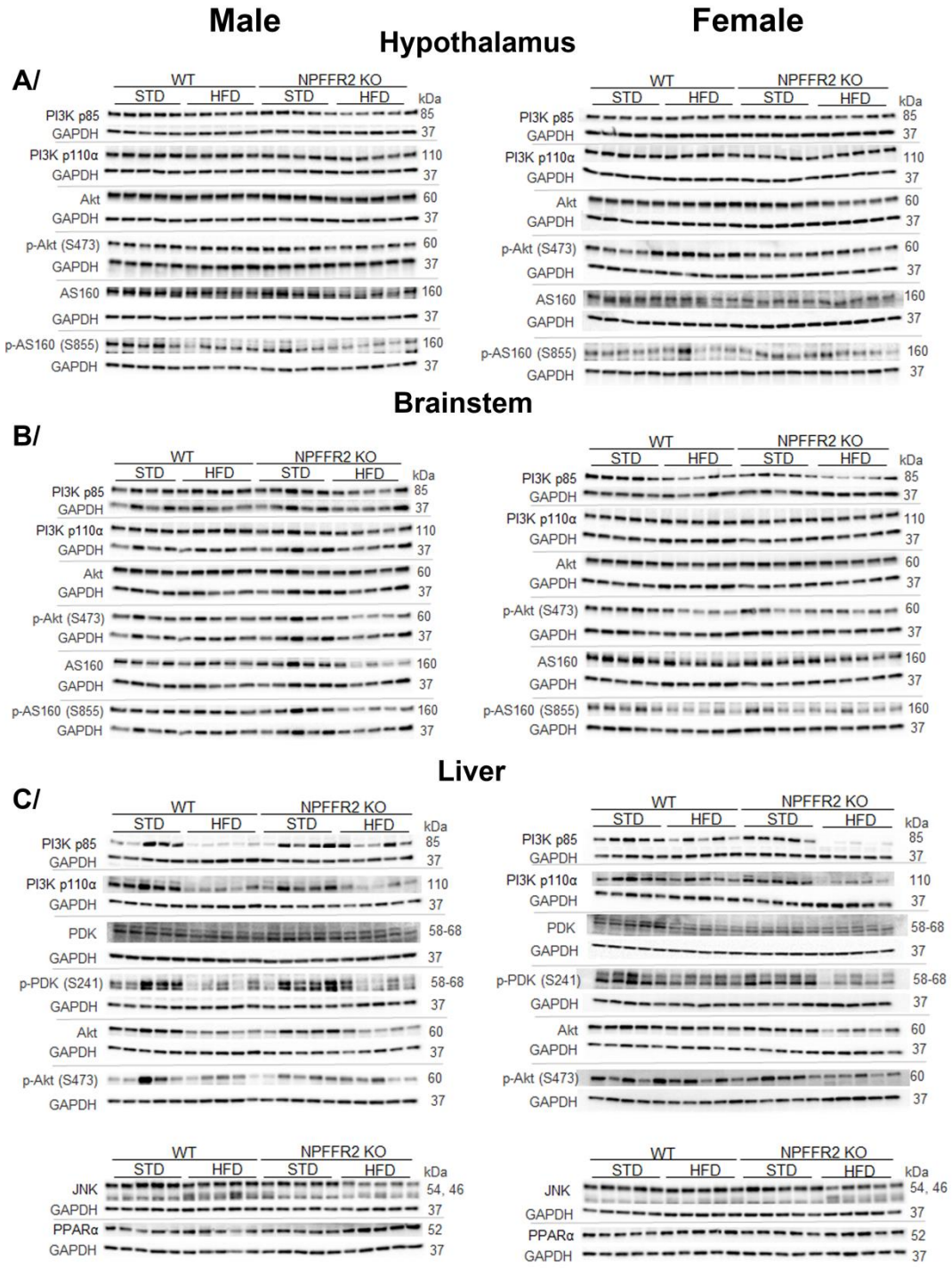

Supplementary Figure 7. Overview of Western Blot analyses from Figures 5, 6 and 7.

WB analysisofhypothalamic (**A**), brainstem (**B**) and liver (**C**) signalingincludingcontrol protein (GAPDH).